

Crosstalk and Competition in Signaling Networks

Michael A. Rowland,[†] Walter Fontana,[§] and Eric J. Deeds^{†*}

[†]Center for Bioinformatics and [‡]Department of Molecular Biosciences, University of Kansas, Lawrence, Kansas; and [§]Department of Systems Biology, Harvard Medical School, Boston, Massachusetts

ABSTRACT Signaling networks have evolved to transduce external and internal information into critical cellular decisions such as growth, differentiation, and apoptosis. These networks form highly interconnected systems within cells due to network crosstalk, where an enzyme from one canonical pathway acts on targets from other pathways. It is currently unclear what types of effects these interconnections can have on the response of networks to incoming signals. In this work, we employ mathematical models to characterize the influence that multiple substrates have on one another. These models build off of the atomistic motif of a kinase/phosphatase pair acting on a single substrate. We find that the ultrasensitive, switch-like response these motifs can exhibit becomes transitive: if one substrate saturates the enzymes and responds ultrasensitively, then all substrates will do so regardless of their degree of saturation. We also demonstrate that the phosphatases themselves can induce crosstalk even when the kinases are independent. These findings have strong implications for how we understand and classify crosstalk, as well as for the rational development of kinase inhibitors aimed at pharmaceutically modulating network behavior.

INTRODUCTION

Signal propagation through a network of interacting proteins is central to a cell's ability to process and respond to stimuli. In most cases, these interactions involve an enzyme (e.g., a kinase) that covalently modifies a substrate and changes its functionality (i.e., activates/deactivates it as an enzyme, or causes translocation to a different compartment). To regulate the signal, another enzyme (e.g., a phosphatase) reverses the modification, restoring the original functionality of the substrate in question. The net activity of these enzymes alters the functional state of the proteins in the network in response to inputs, and the overall state of the network ultimately determines the cellular response.

Intracellular signaling networks are extremely complex in metazoans, which makes it difficult to understand their behavior (1,2). A major source of this complexity is network crosstalk, i.e., the sharing of input signals between multiple canonical pathways (3–7). For example, kinases can often transmit signals to a large number of different targets: Akt can act on at least 18 substrates, and the receptor tyrosine kinases in the EGF/ErbB family can interact with >20 substrates (8,9). Because eukaryotic genomes contain fewer distinct phosphatases than distinct kinases, phosphatases are generally considered more promiscuous, and even with adaptor proteins targeting their activity, they often act on multiple substrates (10). Although it is clear that crosstalk is widespread in mammalian signaling networks, we currently do not have a clear conceptual picture of how this highly interconnected architecture might influence the response of a network to incoming signals.

In this work, we seek to understand how the competition and promiscuity induced by crosstalk ultimately influence

network behavior. In classic crosstalk, a kinase is shared between two pathways and can transfer signals from one pathway to another (3,5,7,11); for instance, mitogen-activated protein kinase (MAPK) networks often use the same enzymes in multiple cascades (12). Most previous computational studies on this subject have focused on characterizing the spatial or temporal mechanisms for the insulation of MAPK signaling cascades despite the potential for crosstalk (13–15). It has been demonstrated, however, that competition among targets of the same kinase can have profound effects on substrate phosphorylation (16). Here, we extend these previous findings to characterize in detail how crosstalk can actively couple the response of multiple proteins to incoming signals. We developed models that consider a set of general motifs, with the goal of understanding how features such as substrate saturation and phosphatase architecture can influence substrate response.

Our models build off a simple futile cycle in which one enzyme modifies a single substrate and another enzyme removes the modification, which we represent as a kinase and phosphatase pair interacting with a target protein (see Fig. 1 A). As first shown by Goldbeter and Koshland (18) over 30 years ago, the fraction of modified substrate for this cycle can be expressed as a function of three parameters:

$$K_K = \frac{K_{m,K}}{[S]_0}, \quad K_P = \frac{K_{m,P}}{[S]_0}, \quad r = \frac{V_{max,K}}{V_{max,P}} \quad (1)$$

where $[S]_0$ is the total amount of substrate, $K_{m,K}$ and $K_{m,P}$ are the Michaelis constants for the two enzymes, K_K and K_P represent the inverse of the degree of saturation of the enzymes, and r is the ratio of their maximum velocities. Detailed definitions of these constants in terms of the underlying rates of the enzymatic reactions can be found in the context of Eq. 2 below. One can easily solve the underlying

Submitted August 16, 2012, and accepted for publication October 10, 2012.

*Correspondence: deeds@ku.edu

Editor: Dennis Bray.

© 2012 by the Biophysical Society
0006-3495/12/12/2389/10 \$2.00

<http://dx.doi.org/10.1016/j.bpj.2012.10.006>

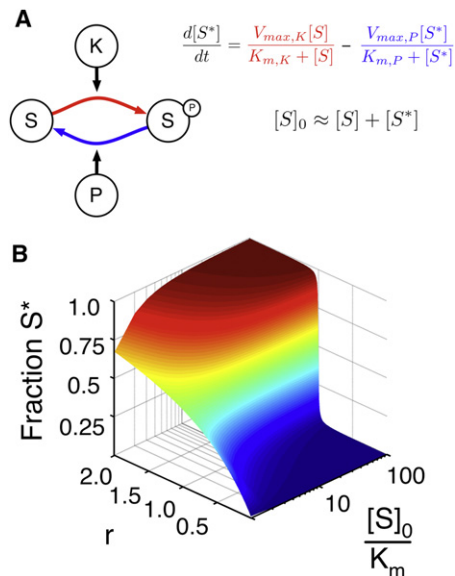


FIGURE 1 The Goldbeter-Koshland loop. (A) A pair of enzymes (say, a kinase K and a phosphatase P) acts on a single substrate. The associated equations show the change in S^* concentration as the difference between the production of S^* by the kinase (in red) and the production of S by the phosphatase (in blue). Here we assume that the concentration of free S and S^* is far greater than the concentrations of bound S in either form, which is necessary to obtain the standard Michaelis-Menten forms for the enzymatic reaction velocities (18). (B) The fraction of phosphorylated S (z axis) is a function of r and $[S]_0$. The total concentration of $[S]$ is normalized by its K_m (which is identical for both the kinase and phosphatase) and is plotted on a log scale.

system of differential equations (see Fig. 1 A) at steady state, providing a relationship between overall substrate phosphorylation and the parameters listed in Eq. 1 (see Eq. 3 below, with $\alpha_{K,1} = \alpha_{P,1} = 1$). Because protein levels tend to change slowly (17), we expect that saturation (and thus K_K and K_P) will remain constant on short timescales during the response to signal. On the other hand, r changes with the concentration of active kinase and phosphatase. Incoming signals generally modulate active K or P concentration, thus making r the dominant response parameter. When the substrate does not saturate the enzymes, phosphorylation of the substrate increases hyperbolically with r . However, when the substrate saturates both enzymes, the loop displays a switch-like behavior in r , referred to as 0th order ultrasensitivity (Fig. 1 B). In this case, at values of $r < 1$ the fraction of phosphorylated substrate is very low, and at $r > 1$ the system switches to a highly phosphorylated state (18). The ultrasensitive response of a substrate at saturating concentrations has been observed experimentally in a number of systems (16,19–23).

We expanded this model to include competing substrates at either or both enzymes to characterize the influence of multiple targets on signaling (Fig. 2, A–C). All three of the motifs we consider are found in well-known signaling systems, such as the Fus3/Cdk1 network in yeast and other

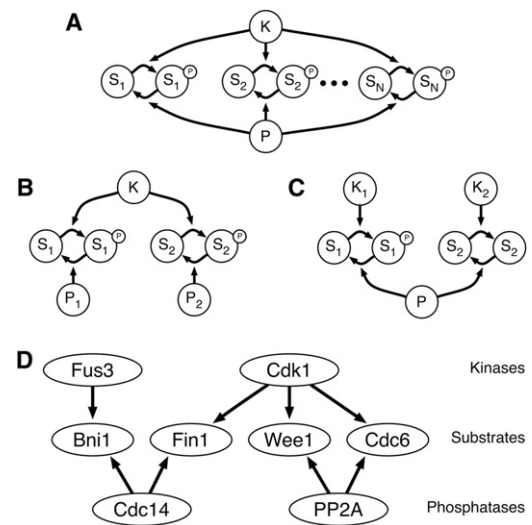


FIGURE 2 Crosstalk schematic. (A) A pair of enzymes (a kinase K and phosphatase P) acting on N substrates; we term this the 1K1P loop. (B) A kinase that has two substrates, each with its own independent phosphatase (P_1 and P_2); we term this the 1K2P loop. (C) Two independent kinases (K_1 and K_2) acting on two substrates that share a single phosphatase P ; we term this the 2K1P loop. (D) A section of the yeast Cdk1 signaling network, including each of these three motifs (16,44–49). Although the interactions shown are specific to yeast, there are human homologs for each of the proteins listed. The full network in this case contains a number of downstream feedback mechanisms that are omitted for clarity. These mechanisms may be abrogated by mutations so that the local influence of competition can be studied experimentally (16). The competition between Wee1 and Cdc6 is an example of the 1K1P loop, whereas Wee1 and Fin1 form a 1K2P loop, and Fin1 and Bni1 form a 2K1P loop.

eukaryotes (Fig. 2 D). We found that shared signaling enzymes can couple the responses of different substrates. For instance, when there is more than one substrate of the same kinase and phosphatase (see Fig. 2 A), if one substrate is at sufficient concentration to elicit an ultrasensitive response, then all substrates that share the pair enzymes in the cycle will exhibit ultrasensitivity without necessarily saturating the enzyme themselves. We have shown that in systems in which two substrates share a phosphatase (see Fig. 2 C), one substrate saturating the phosphatase can cause the other substrate to ultrasensitively respond to signals from the first kinase. This indicates a novel potential for phosphatases to be involved in network crosstalk.

Kinases are becoming increasingly popular drug targets in the treatment of cancer and other diseases (24). We considered how such inhibitors might influence the behavior of these various crosstalk architectures, and found that these inhibitors can have important consequences that would be difficult to predict in the absence of a detailed understanding of network topology and enzyme saturation.

Overall, our work demonstrates that enzymes with multiple targets can couple signal responses, and that systems considered in a cellular context may exhibit behaviors vastly different from those considered in isolated models. These results have implications for how we understand the role

of crosstalk in signaling, and how we can potentially control the propagation of the effects of enzymatic inhibitors through highly connected networks.

MATERIALS AND METHODS

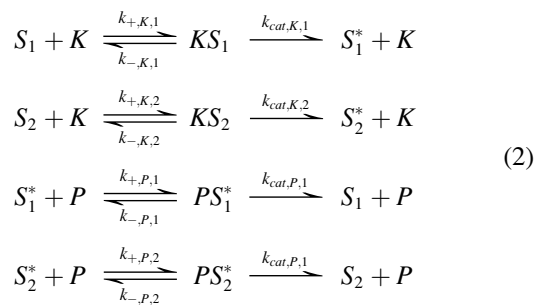
The behaviors of each model are described by sets of ordinary differential equations (ODEs), which are written explicitly for each system in section 1 of the [Supporting Material](#). The systems of ODEs were numerically integrated using the CVODE package from SUNDIALS (25). We employed the dense linear solver with the backward differentiation formula and a Newton iteration methodology available in that package for all of the dynamics discussed in this work. The values of the parameters used in each case are included in the [Supporting Material](#).

Steady-state measurements were obtained by allowing the system to run until the level of each species of the system stabilized. The actual times at which the measurements were made were chosen heuristically by visual inspection of the trajectories themselves. The surfaces obtained in [Figs. 3](#) and [4](#) were confirmed analytically by solving for S_1^* in the same manner as described by Goldbeter and Koshland (18). The analytical results are derived in sections 2–4 of the [Supporting Material](#).

RESULTS

1-Kinase/1-phosphatase loop with two substrates

We first considered a signaling motif in which a kinase (K) and phosphatase (P) act on multiple substrates, which we term the 1-kinase/1-phosphatase (1K1P) loop. An example of this can be found in yeast, where the proteins Wee1 and Cdc6 compete for both the kinase Cdk1 and phosphatase PP2A ([Fig. 2 D](#)). In the simplest case, we included two substrates of the kinase and phosphatase, S_1 and S_2 , each of which can exist in an unphosphorylated and phosphorylated (e.g., S_1^*) form (see [Fig. 2 A](#), $N = 2$). The set of enzymatic reactions is as follows:



Each of the above reactions involves three elementary rates: the rate of complex formation (k_+), the rate of complex dissociation (k_-), and the enzyme catalytic rate (k_{cat}). From these rates we can obtain the Michaelis constant for

both enzymes: $K_{m,K,i} = (k_{-,K,i} + k_{cat,K,i})/k_{+,K,i}$ and $K_{m,P,i} = (k_{-,P,i} + k_{cat,P,i})/k_{+,P,i}$. Additionally, we can define the maximum velocity of each enzymatic reaction as $V_{max,K,i} = [K]_0 k_{cat,K,i}$ and $V_{max,P,i} = [P]_0 k_{cat,P,i}$. Each kinase and phosphatase molecule can only bind and act on one substrate at any given moment, and as such, S_2 acts as a competitive inhibitor of the kinase and phosphatase reactions with S_1 . This results in a set of inhibitory constants, $\alpha_{K,1} = 1 + [S_2]/K_{m,K,2}$ and $\alpha_{P,1} = 1 + [S_2^*]/K_{m,P,2}$, that capture the effects of S_2 on the S_1 kinase and phosphatase reactions, respectively. S_1 inhibition of the S_2 reactions generates similar constants, $\alpha_{K,2}$ and $\alpha_{P,2}$ (see the [Supporting Material](#)). The fact that multiple targets constitute competitive inhibitors of each other has been observed experimentally for both kinases and phosphatases (16,26,27). These α terms are identical to what one would obtain for a generic competitive inhibitor, $\alpha = 1 + [I]/K_I$ (28). Where the activity of a generic inhibitor against its target enzyme depends solely on its concentration, a competitive substrate will inhibit either the kinase or the phosphatase based on the concentrations of its unphosphorylated and phosphorylated forms, respectively. Because these concentrations are controlled by incoming signals, mutual inhibition has the potential to couple substrate responses.

The chemical reactions in [Eq. 2](#) can be readily used to define a system of ODEs in which the binding, dissociation, and catalysis steps are treated explicitly (see the [Supporting Material](#)). We numerically integrated these equations and calculated the fraction $S_1^* \equiv [S_1^*]/[S_1]_0$ at steady state at various concentrations of S_2 for a case in which S_1 does not saturate the enzymes. In this work, we consider a case in which the saturation of all enzymes by any given substrate is equal; we leave the case of differential saturation among enzymes (12) to future studies. The response of the system is controlled by two r values, r_1 and r_2 , which are the ratios of the maximum velocities of the enzymes with respect to either substrate. The results of these calculations are summarized in [Fig. 3 A](#). As expected, when there is no S_2 present to compete with S_1 for the enzymes, S_1^* increases as a rectangular hyperbola in r_1 . When S_2 saturates the enzymes, however, we find that S_1 displays an ultrasensitive response in r_1 in a fashion similar to the ultrasensitive response obtained by increasing S_1 concentration in [Fig. 1 B](#).

These findings can be understood by treating the 1K1P loop analytically. In the limit in which the total concentration of the substrates is much larger than the total concentration of either enzyme (i.e., $[S_i]_0 \approx [S_i] + [S_i^*]$), we can calculate the fraction S_1^* as

$$S_1^* = \frac{(r_1 - 1) - (\alpha_{K,1}K_{K,1} + \alpha_{P,1}r_1K_{P,1}) + \sqrt{((r_1 - 1) - (\alpha_{K,1}K_{K,1} + r_1\alpha_{P,1}K_{P,1}))^2 + 4(r_1 - 1)r_1\alpha_{P,1}K_{P,1}}}{2(r_1 - 1)} \tag{3}$$

which is identical to the original result of Goldbeter and Koshland (18) except for the α inhibition terms (see the [Supporting Material](#) for details about the solution). Note that S_1^* depends on $[S_1]_0$ through the K terms as well as $[S_2]$ and $[S_2^*]$ through the α terms. The equation for S_2^* is identical to Eq. 3 with a change of indices. This result is a generalization of previous findings on multiple substrates in a Goldbeter-Koshland loop, allowing for both kinase saturation and saturation of a shared phosphatase (16). When $[S_1]_0 \ll K_m$, as in Fig. 3 A, $\alpha_{K,2} \approx 1$ and $\alpha_{P,2} \approx 1$. In this case, S_2 will behave as an isolated Goldbeter-Koshland loop and as such will display an ultrasensitive response in r_2 when $[S_2]_0 \gg K_m$. Because incoming signals vary r by changing the relative concentrations of active enzymes, $r_1 \propto r_2$ (for purposes of display in Fig. 3 A, we assumed $r_1 = r_2$). When $r_2 < 1$, S_2 will be largely unphosphorylated and will inhibit the kinase's action on S_1 , causing S_1 to be primarily in its unphosphorylated state. Similarly, when $r_2 > 1$, S_2 will be mostly phosphorylated and will inhibit the S_1 dephosphorylation reaction by saturating the phosphatase. In combination, this coupling transfers the ultrasensitive response of S_2 to the S_1 curve. We have proven mathematically that an increase in S_2 ultrasensitivity (i.e., increasing S_2 concentration) always increases the ultrasensitivity of the response of S_1 in r_2 regardless of the values of the kinetic parameters (see the [Supporting Material](#)). The general behavior observed in Fig. 3 A is thus a qualitative feature of all 1K1P loops.

It has been shown experimentally that the competition between multiple phosphorylation sites on the protein Wee1 contributes to the ultrasensitivity of Wee1's response to incoming signals (16). Although multisite phosphorylation can have a number of influences on such systems (e.g., by introducing thresholds or bistability (2,29,30)), these findings are consistent with the predictions made by Eq. 3.

1K1P with many substrates

We further developed the 1K1P loop to include $N > 2$ substrates of the kinase and phosphatase (see Fig. 2 A). As described above, we numerically integrated the resulting ODEs and calculated the fraction S_1 at steady state in a case in which we include a varying number of substrates, each of which does not saturate the enzymes. The results of these calculations are summarized in Fig. 3 B. As expected, S_1^* increases as a rectangular hyperbola in r_1 in the absence of other substrates. As new unsaturating substrates are added to the system, we see that S_1^* starts to show an ultrasensitive response in r_1 , even though none of the substrates are at a concentration that would produce such a response on their own.

Once again, these results can be understood by treating the loop analytically. In this case, the collection of substrates act

as competitive inhibitors of the S_1 loop. As such, the inhibitory constants must now account for all competing substrates and can be expressed as $\alpha_{K,1} = 1 + \sum_{i=2}^N [S_i]/K_{m,K,i}$ and $\alpha_{P,1} = 1 + \sum_{i=2}^N [S_i^*]/K_{m,P,i}$ (see the [Supporting Material](#) for the derivation). Considering the case in which $N > 2$ reveals that saturation of the enzymes can be the combined result of many substrates, rather than one substrate saturating the enzymes on its own. When the kinase is saturated by any subset of its targets, S_1 's kinase reaction is inhibited, and a similar inhibition occurs with the phosphatase. Thus, given enough substrates, the entire system can show ultrasensitivity in r_1 even when none of the substrates individually saturate the enzymes.

As mentioned in the Introduction, kinases often have multiple targets within cells; for instance, Cdk1 has hundreds of substrates in yeast (2,31,32), and the ErbB receptor tyrosine kinases in humans have between 20 and 40 potential targets. In the latter case, the K_D values measured by Kaushansky et al. (33) indicate that the 1 μ M K_M value used in generating Fig. 3 is a reasonable estimate. The collective-saturation mechanism described above may thus represent a common scenario for generating ultrasensitivity in substrate response.

1-Kinase/2-phosphatase loop

Most of our empirical understanding of crosstalk comes from studies that focused on the motif of a kinase with more than one substrate (34). Because the specific phosphatases that act on any given set of targets are often not known, it is not clear that all kinase crosstalk will follow the 1K1P pattern discussed above (Fig. 2 A). For instance, Fin1 and Wee1 share the same kinase (Cdk1) but have separate phosphatases (Cdc14 and PP2A, respectively; Fig. 2 D). Also, because kinases often have a very large number of targets, systems in which substrates share the same kinase but possess separate phosphatases may be widespread (8,9,31,32). As such, we considered the behavior of the 1-kinase/2-phosphatase (1K2P) loop as diagrammed in Fig. 2 B. In this case, because the phosphatases are independent, we can separate the r parameters (i.e., $r_2 \neq r_1$). At low substrate concentrations, S_1 responds hyperbolically in r_1 and is insensitive to r_2 (Fig. 4 A). When $[S_2]_0 \gg K_m$ and $r_2 < 1$, S_1 phosphorylation is greatly reduced (Fig. 4 B). In fact, one observes very little S_1 phosphorylation until $r_2 > 1$. In contrast to the 1K1P loop, the response of S_1 to r_2 thus exhibits a threshold: when $r_2 < 1$, S_1 essentially cannot respond to signals. At values of $r_2 > 1$, however, S_1 responds hyperbolically to both r_1 and r_2 .

The fraction S_1^* for the 1K2P loop also follows Eq. 3, but with $\alpha_{P,1} = 1$ because the phosphatases are independent. The presence of S_2 in the system thus generally decreases the phosphorylation level of S_1 (compare Fig. 4, A and B). The thresholding behavior seen in Fig. 4 B occurs because the concentration of the inhibitor

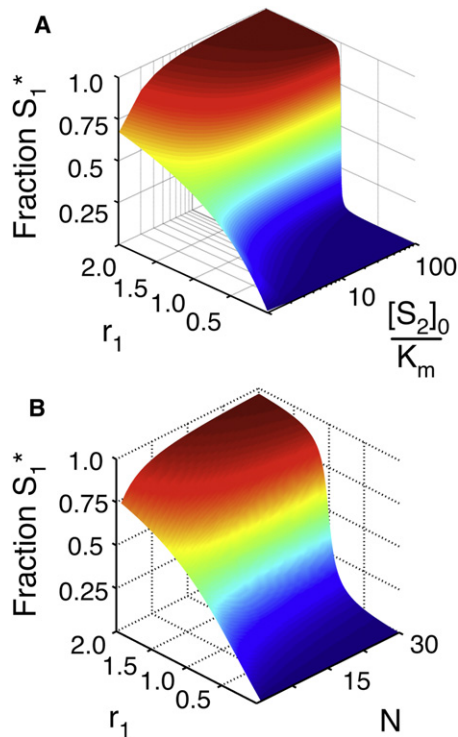


FIGURE 3 Results for the 1K1P loop. (A) The fraction of phosphorylated S_1 (z axis) as a function of r_1 and $[S_2]_0$. Note that for the purpose of display, we have set $r_1 = r_2$ in this case. The total concentration of $[S_2]$ is normalized by its K_m (which is identical for both the kinase and phosphatase) and is plotted on a log scale. (B) The fraction of phosphorylated S_1 as a function of r_1 and the number of additional substrates in the loop (N , see Fig. 2 A). All substrates are below saturating concentrations ($[S_i]_0 = 0.1 \times K_m$). As in A, for the purpose of display, the r and K_m parameters have been set to be equal for all substrates. Note that in both panels A and B, the fraction S_1^* responds to r_1 with increasing ultrasensitivity as the total saturation of the enzymes (represented by $[S_2]_0/K_m$ or N , respectively) increases.

(i.e., unphosphorylated S_2) responds ultrasensitively to r_2 . If $r_2 < 1$, the inhibitor concentration is high, and no phosphorylation of S_1 can take place. At $r_2 > 1$, the inhibitor is largely removed from the system, allowing S_1 to respond to incoming signals. However, it is only in the limit $r_2 \rightarrow \infty$ (i.e., $\alpha_{K,1} \rightarrow 1$) that S_1 will behave as an isolated futile cycle. As with the 1K1P loop, we have shown mathematically that addition of S_2 always decreases S_1^* regardless of the values of the parameters in the limit $S_1^* \ll K_m$ (see the Supporting Material). This indicates that the gatekeeper function played by S_2 is a robust feature of 1K2P loops.

Kim and Ferrell (16) showed experimentally that adding Fin1 and Cdc6 to *Xenopus* cell extracts increases the active kinase concentration (i.e., r) required to induce a Wee1 response. Although the experiment in this case involves both a 1K1P and a 1K2P loop (Fig. 2 D), these findings are consistent with our prediction that competitive substrates tend to decrease the phosphorylation levels of other targets when the phosphatase is not shared.

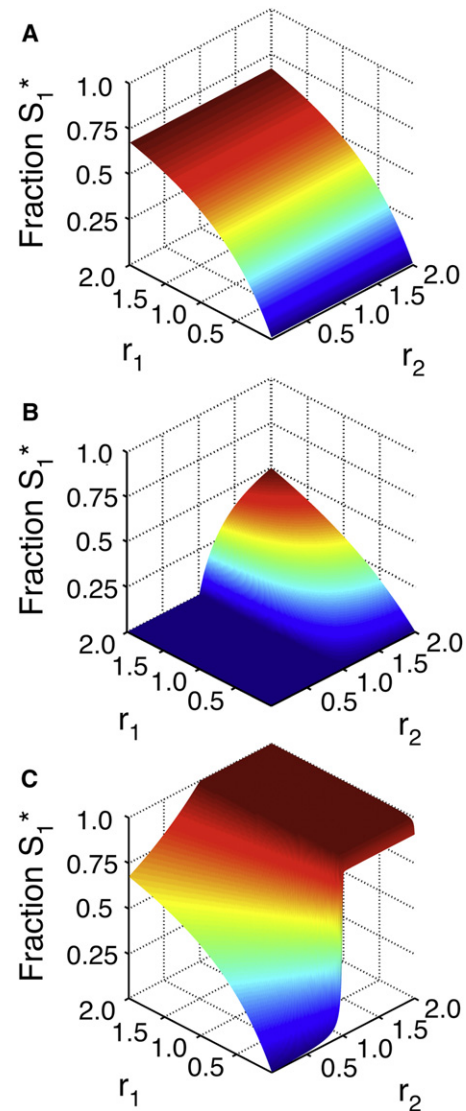


FIGURE 4 Influence of phosphatase architecture on network response. (A) The fraction of phosphorylated S_1 as a function of r_1 and r_2 when $[S_2]_0 \ll K_m$ for both the 1K2P and 2K1P loops. In this case, $[S_1]_0 = 0.1 \times K_m$. Note that r_2 has little effect on the response of the S_1 loop. (B) The fraction of phosphorylated S_1 as a function of r_1 and r_2 for a 1K2P loop with $[S_2]_0 = 20 \times K_m$. As in A, $S_1 = 0.1 \times K_m$. If S_2 saturates the enzymes, it becomes a gatekeeper; when $r_2 < 1$ (i.e., when the S_2 loop is switched to the unphosphorylated state), the S_1 loop essentially cannot respond to incoming signals. When $r_2 > 1$, however, S_1^* responds hyperbolically in both r_1 and r_2 . (C) The fraction of phosphorylated S_1 as a function of r_1 and r_2 for a 2K1P loop. As in B, $[S_1]_0 = 0.1 \times K_m$ and $[S_2]_0 = 20 \times K_m$. Saturating concentrations of S_2 generally increase phosphorylation in this case. Note that even when $r_1 \ll 1$, S_1 shows an ultrasensitive response to r_2 (and thus K_2) despite receiving only basal levels of signal from its own kinase. This indicates the potential for significant phosphatase crosstalk in signaling networks.

2-Kinase/1-phosphatase loop

The human genome encodes ~ 150 catalytically active phosphatases and phosphatase domains, and almost 500 kinases (35,36). As such, phosphatases are generally considered

promiscuous; although adaptor proteins help increase phosphatase specificity, these complexes still can target multiple substrates (10). Because of this promiscuity, it is reasonable to imagine that motifs in which two substrates share a single phosphatase but are phosphorylated by independent kinases are relatively common arrangements in signaling networks. There are certainly examples of such situations: for instance, Fin1 and Bni1 in yeast share a phosphatase (Cdc14) but have different kinases (Cdk1 and Fus3, respectively; Fig. 2 D). We used the 2-kinase/1-phosphatase (2K1P) loop as modeled in Fig. 2 C to characterize the behavior of such systems. As with the 1K2P loop, the distinct kinases in the 2K1P system allow the separation of r parameters so that $r_1 \neq r_2$.

At low substrate concentrations, this is essentially the case. As anticipated, S_1 responds hyperbolically in r_1 and is insensitive to r_2 (see Fig. 4 A). The situation is very different when $[S_2]_0 \gg K_m$. We see the expected hyperbolic S_1 response in r_1 when r_2 is nearly zero (i.e., when the S_2 loop has not received an activation signal); however, as r_2 increases, the fraction of phosphorylated S_1 molecules increases until it reaches nearly one at $r_2 > 1$ (Fig. 4 C). When r_1 is close to zero, S_1 responds ultrasensitively to r_2 . This indicates that a signal that switches S_2 to its phosphorylated state can cause a similar switch in S_1 even if very little signal is received via K_1 .

As with the 1K1P loop, this behavior can be explained in terms of the inhibition of one loop by another. In this case, the fraction S_1^* can be defined as in Eq. 3 with $\alpha_{K,1} = 1$ to account for the independence of the kinases. Adding S_2 to the system thus generally increases phosphorylation of S_1 (compare Fig. 4, A and C). Because phosphorylated S_2 acts as a phosphatase inhibitor, an incoming signal that increases r_2 to values greater than one introduces high concentrations of the inhibitor in a switch-like manner, inducing a response in S_1 . We have shown mathematically that this increase in phosphorylation in response to S_2 competition will always occur regardless of parameters in the limit $S_1^* \ll K_m$ (see the Supporting Material).

Phosphatase tunneling

In the models described above, we focused on crosstalk occurring between substrates on the same level of signaling; the only relationship between the substrates is the shared enzymes. Signaling networks, however, often contain cascades in which a set of proteins activate each other in sequence (37). Although the sharing of phosphatases between different levels of a cascade has been documented (6), the phosphatase architecture in these cases is often poorly understood. Indeed, anonymous and independent phosphatases are often added to mathematical models of MAPK cascades to fill in these gaps (21,38–40). Given this ambiguity, we constructed models of cascades in which each kinase has an independent phosphatase, in addition to a

case in which a single phosphatase acts on all of the proteins in the cascade (Fig. 5, A and B).

Each type of cascade was modeled with depth $N = 2, 3, 4$, or 5 substrates present in saturating ($10 \times K_m$) or unsaturating ($0.1 \times K_m$) concentrations. The input parameter r was defined as the ratio of the maximum velocities of the initial kinase (K) to the phosphatase acting on S_1 (P_1 or P for the independent and shared cases, respectively), and the models were analyzed for the fraction of the final substrate phosphorylated (S_N^*) at steady state.

For both classes of cascade, we found that the response of the final substrate becomes exponentially more sensitive to input signals with increasing cascade depth. The $N = 5$ case generally reaches its $r_{1/2}$ (the r -value at which half of S_N is phosphorylated) with 9 orders of magnitude less input

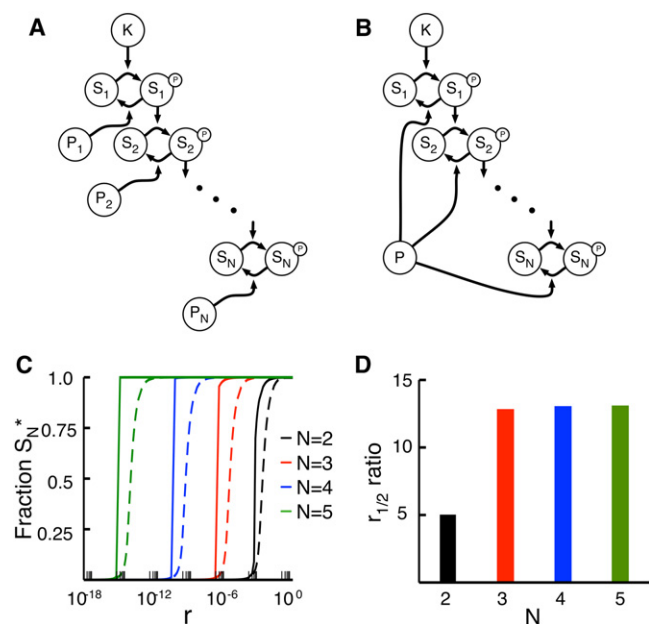


FIGURE 5 Influence of phosphatase tunneling on cascade signals. (A) A kinase cascade with N members. The kinase K provides the input signal, and each substrate S_i acts as the kinase for substrate S_{i+1} . In this model, there are N independent phosphatases (P_i). This expands upon systems previously described by Goldbeter and Koshland (18). (B) A kinase cascade similar to that in panel A, but with a single shared phosphatase P . (C) Fractional phosphorylation of the final substrate in the cascade as a function of r for cascades with two to five substrates. In this case, r is defined as the V_{max} of the input kinase (K in A and B) divided by the V_{max} of the phosphatase for the first substrate in the cascade (P_1 in A, and P in B). The dashed lines represent cascades with N phosphatases and the solid lines represent cascades with a single shared phosphatase. Note that the responses of cascades become exponentially more sensitive to r with increasing depth N . Cascades with a single shared phosphatase are considerably more sensitive to r compared with those with independent phosphatases. (D) In this case, we define a parameter, $r_{1/2}$, as the value of r in panel C at which the response of a cascade is half-maximal. For any given number of substrates, N , the $r_{1/2}$ ratio is the $r_{1/2}$ of the independent case divided by the $r_{1/2}$ of the shared case (i.e., the $r_{1/2}$ of the dashed curve in C divided by the $r_{1/2}$ for the solid curve). For $N = 2$, the independent case requires ~ 5 times as much input signal to achieve a half-maximal response; for $N = 3, 4$, and 5, the independent case requires ~ 13 times as much input signal.

than $N = 2$ (see Fig. 5 C). This increase in sensitivity is an expected outcome of amplification in signaling cascades (18,41). Additionally, models with a single, shared phosphatase show a higher degree in input sensitivity in r compared with models with independent phosphatases, but only when the substrates are present at saturating concentrations.

To quantify the changes in input sensitivity for saturating conditions, we took the ratio of the $r_{1/2}$ -values for the two types of cascade at a given value of N (see Fig. 5 D). In the most basic cascade, with $N = 2$, the $r_{1/2}$ for the single phosphatase model is ~ 5 times less than that for the multiple phosphatase model. This ratio increases and plateaus for cascades with depth $N \geq 3$; in these cases, the single phosphatase models require ~ 13 times less signal. This occurs because the signal is able to tunnel through the shared phosphatase when the substrates are at saturating concentrations. Activation of the upstream kinases not only activates the rest of the cascade but also produces phosphorylated substrate molecules that act as phosphatase inhibitors. This reduces the effective concentration of free phosphatase available for downstream substrates, amplifying the apparent signal strength.

Kinase inhibitors

As mentioned above, there is a growing interest in developing small molecules that target and inhibit kinases as potential therapeutics for a variety of diseases (24). It is unclear, however, what kind of effects these inhibitors will have in loops with significant kinase or phosphatase crosstalk; in these cases, kinase inhibitors not only influence their targets' activity but also the concentration of other inhibitors (namely, S_2 and S_2^*) in the system. We considered the impact of two separate types of inhibitors on the loops described above. Type 1 inhibitors, which are currently by far the most commonly used in practice (24), target the ATP-binding site of a specific kinase and disrupt its activity toward all of its targets. Type 2 inhibitors, on the other hand, target and disrupt a specific kinase–target interaction, leaving the kinase free to act on a subset of its other targets. Although the latter is not currently common, peptide inhibitors have been successfully used in this manner (27), and there is increasing interest in developing the capacity to inhibit specific protein–protein interactions within cells (42).

We modeled the potential effects of these inhibitors by including explicit inhibitor molecules in our loops, with I_1 and I_2 representing type 1 and type 2 inhibitors, respectively. We first considered a 1K1P loop with S_2 at saturating concentrations and in the active state ($r_1 = r_2 = 1.5$; see Fig. 2 A). As one would expect, adding I_1 significantly decreases S_1^* , because a generic inhibitor for the kinase will clearly reduce overall phosphorylation of all targets (Fig. 6 A). However, even an inhibitor that is specific to S_2 decreases the phosphorylation of S_1 (Fig. 6 A). The specific inhibitor in this case decreases the concentration of

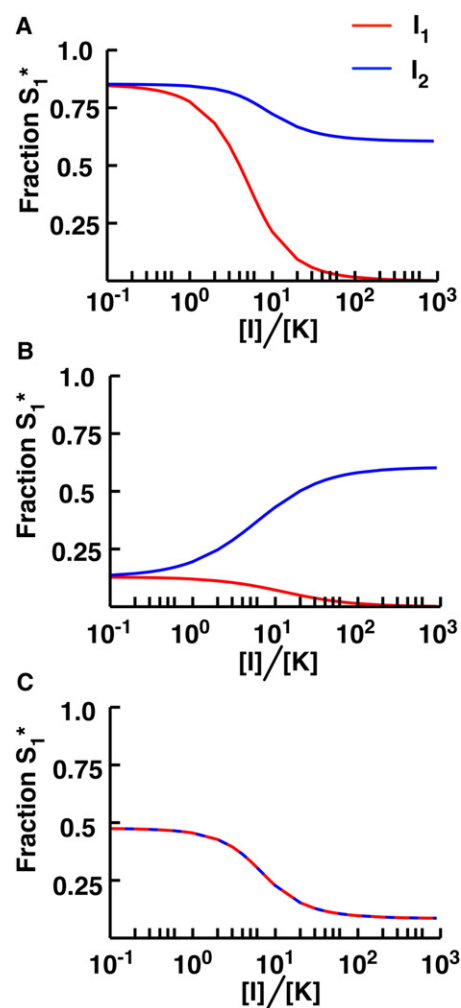


FIGURE 6 Effect of kinase inhibitors in the presence of crosstalk. (A) A 1K1P loop with two substrates in the presence of one of two kinase inhibitors: I_1 , which prevents reactions with all targets of the kinase (red), or I_2 , which specifically disrupts K - S_2 interactions (blue). We plot the fraction of phosphorylated S_1 against the ratio of $[I_1]$ or $[I_2]$ to $[K]$. In this case, $[S_1]_0 = 0.1 \times K_m$, $[S_2]_0 = 20 \times K_m$ and $r_1 = r_2 = 1.5$. Note that using either inhibitor causes a decrease in the fraction S_1^* , although the effect is less pronounced with the S_2 -specific inhibitor. In the latter scenario, I_2 reduces the $[S_2^*]$, which is itself a phosphatase inhibitor for S_1^* . The net effect of I_2 is thus to decrease S_1 phosphorylation. (B) A 1K2P loop with the same kinase inhibitors as in panel A. The fraction of phosphorylated S_1 is plotted against the ratio of $[I_1]$ or $[I_2]$ to $[K]$. In this case, $[S_1]_0 = 0.1 \times K_m$, $[S_2]_0 = 20 \times K_m$, $r_1 = 0.5$ and $r_2 = 1.5$. Although the general inhibitor still reduces S_1^* , the specific inhibitor increases S_1^* . This is because decreasing the concentration of S_2^* reduces competition for the shared kinase. (C) A 2K1P loop in the presence of both I_1 and I_2 . Note that because the kinases are independent in this case, the effects of both inhibitors are identical. The fraction of phosphorylated S_1 is plotted against the ratio of the concentrations of $[I_2]$ to $[K]$. In this case, $[S_1]_0 = 0.1 \times K_m$, $[S_2]_0 = 20 \times K_m$, $r_1 = 0.01$ and $r_2 = 1.5$. Both inhibitors decrease S_1^* , as the reduction in phosphorylated S_2 due to the inhibitors reduces S_2^* 's inhibition of the S_1 phosphatase reaction.

S_2^* , reducing competition for the phosphatase and thus decreasing S_1^* . The effect of I_2 is not as dramatic as that of I_1 for the 1K1P loop, but this nonetheless represents a

potentially unintended consequence of a (putatively) specific inhibitor.

In the 1K2P case, we find exactly the opposite behavior: whereas I_1 decreases S_1^* as expected, I_2 increases the phosphorylation of the first substrate (Fig. 6 B). This is because the inhibitor reduces S_2 interactions with the kinase, alleviating competition. In this case, the response of the system is perhaps more intuitive: because S_2 is a competitive inhibitor of S_1 phosphorylation, inhibiting its phosphorylation in a specific way increases the capacity of S_1 to respond to signals.

In the 2K1P loop, if the two types of inhibitors are aimed at the second kinase (K_2), they have the same net effect. Because K_2 cannot act on S_1 in this model, there is no difference between an inhibitor that simply targets K_2 and one that specifically targets the K_2 - S_2 interaction. When the second loop is activated by a signal and the first loop is not, the K_2 inhibitor completely abolishes S_1 phosphorylation (Fig. 6 C). Although the source of this behavior is clear from Fig. 4 C, the effect is nonetheless striking. In the absence of knowledge about the shared phosphatase (or the phenomenology of the 2K1P loop), a response like the one shown in Fig. 4 C might lead to the erroneous conclusion that K_2 acts directly on S_1 , or that the inhibitor in this case is nonspecific.

DISCUSSION

The 1K1P and 1K2P loops discussed above (Fig. 2, A and B) represent two variations on the classic crosstalk motif, i.e., a kinase that has multiple downstream targets in different pathways. In the traditional view, the coupling between the substrates in these two loops is understood as simply arising from the fact that they will all respond to some of the same upstream signals (34). Our work reveals that a shared enzyme not only modifies each target but also can strongly couple the response of one target to that of another through competitive inhibition at the shared enzyme. For instance, if the targets in question share the same phosphatase, we find that 0th-order ultrasensitivity becomes transitive; all of the targets in this case will respond in a switch-like manner to incoming signals (Fig. 3 A). We also find that in situations where there are a large number of substrates (Fig. 3 B), the system can respond ultrasensitively even if none of the targets is at a high enough concentration to elicit such a response on its own (Fig. 3 B). It has been shown that some kinases do in fact act on many targets (e.g., Akt, the EGF receptors, and Cdk1 (8, 9, 31, 32)), indicating that this collective saturation may represent a common mechanism for inducing ultrasensitivity without having to express any given protein target at saturating levels.

We find that the alternative variation on traditional kinase crosstalk, the 1K2P loop (Fig. 2 B), displays a completely different set of behaviors from those observed when the

phosphatase is shared. In this case, the saturating substrate acts as a type of gatekeeper for the other substrates in the loop. Below the signal threshold at which this saturating substrate switches into the phosphorylated state, other substrates will simply be unable to respond to incoming signals, whereas above this threshold the unsaturating targets will respond in a hyperbolic manner (Fig. 4 B). Although direct experimental tests are currently lacking, our predictions for both 1K1P and 1K2P loops are consistent with available data (16). Overall, these findings indicate that when a particular kinase has multiple targets in multiple pathways, it is difficult to reason in general about the behavior of the system in the absence of detailed information regarding phosphatase architecture and relative saturation levels (Figs. 3 and 4).

To date, nearly all experimental characterizations of crosstalk have focused on kinases, and, to our knowledge, the potential for phosphatases to couple signaling responses on their own has not been previously considered (34). Our analysis of the 2K1P loop (Fig. 2 C) demonstrates that such coupling is readily achieved. Indeed, a shared phosphatase can elicit an ultrasensitive response of a target to signals from kinases that do not directly act on the target in question (Fig. 4 C). Furthermore, phosphatase architecture plays a role in the sensitivity of a signaling cascade. We found that cascades in which every substrate shares a common phosphatase are more responsive to input signals than cascades with independent phosphatases when the substrates are at saturating levels. Given that phosphatases are generally considered more promiscuous than kinases, this indicates that phosphatase crosstalk may be widespread in biological networks. Because the specific phosphatases that act on many targets in signaling networks are often not known (38–40), it is currently unclear to what extent phosphatase crosstalk can influence global network behavior.

Given the widespread crosstalk present in mammalian signaling networks, our work highlights the inherent difficulty of predicting a priori the effects that kinase inhibitors will have on cells. These effects ultimately will depend not only on the kinase connectivity of the network but also on the degree of saturation in the targets and the phosphatase architecture. In many cases, both of these facts are unknown—even if the intracellular concentrations of the target proteins are known, the K_m -values for kinases and (especially) phosphatases are not known, and for many signaling pathways the relevant phosphatases have not yet been identified. Understanding these details will be a crucial component of any attempt to rationally design a kinase inhibition strategy that can elicit some desired effect on some set of targets without inducing unintended decreases (or increases) in the phosphorylation levels of other proteins in the network (Fig. 6).

Ultimately, our work indicates that studies on signaling and regulatory networks need to be increasingly mindful

of the highly interconnected and interdependent structure of the networks themselves. This is especially true of phosphatases. To understand the real consequences of rampant kinase crosstalk, we clearly must obtain more reliable information about which phosphatases act on which targets, what adaptor domains they employ, etc. The findings described above also highlight the fact that individual elements of signaling networks can exhibit responses that are sensitive to the context in which the element is found. Care must be taken to ensure that this dependence on network architecture informs our interpretation and understanding of how networks function and interact with each other.

SUPPORTING MATERIAL

Additional equations, results, and reference (43) are available at [http://www.biophysj.org/biophysj/supplemental/S0006-3495\(12\)01109-5](http://www.biophysj.org/biophysj/supplemental/S0006-3495(12)01109-5).

The authors thank Tom Kolokotronis, Van Savage, Dan Yamins, Javier Apfeld, Catalina Romero, Nick Stroustrup, and Deborah Marks for many helpful discussions. We thank Ryan Suderman, Dustin Maurer, and Zaikun Xu for their comments on the manuscript.

REFERENCES

- Mayer, B. J., M. L. Blinov, and L. M. Loew. 2009. Molecular machines or pleiomorphic ensembles: signaling complexes revisited. *J. Biol.* 8:81.
- Thomson, M., and J. Gunawardena. 2009. Unlimited multistability in multisite phosphorylation systems. *Nature*. 460:274–277.
- Danielpour, D., and K. Song. 2006. Cross-talk between IGF-I and TGF- β signaling pathways. *Cytokine Growth Factor Rev.* 17:59–74.
- Hill, S. M. 1998. Receptor crosstalk: communication through cell signaling pathways. *Anat. Rec.* 253:42–48.
- Javelaud, D., and A. Mauviel. 2005. Crosstalk mechanisms between the mitogen-activated protein kinase pathways and Smad signaling downstream of TGF- β : implications for carcinogenesis. *Oncogene*. 24:5742–5750.
- Junttila, M. R., S. P. Li, and J. Westermarck. 2008. Phosphatase-mediated crosstalk between MAPK signaling pathways in the regulation of cell survival. *FASEB J.* 22:954–965.
- Liu, Q. H., and P. A. Hofmann. 2004. Protein phosphatase 2A-mediated cross-talk between p38 MAPK and ERK in apoptosis of cardiac myocytes. *Am. J. Physiol. Heart Circ. Physiol.* 286:H2204–H2212.
- Brazil, D. P., and B. A. Hemmings. 2001. Ten years of protein kinase B signalling: a hard Akt to follow. *Trends Biochem. Sci.* 26:657–664.
- MacBeath, G. 2002. Protein microarrays and proteomics. *Nat. Genet.* 32 (Suppl):526–532.
- Virshup, D. M., and S. Shenolikar. 2009. From promiscuity to precision: protein phosphatases get a makeover. *Mol. Cell.* 33:537–545.
- Eliceiri, B. P. 2001. Integrin and growth factor receptor crosstalk. *Circ. Res.* 89:1104–1110.
- Gomez-Uribe, C., G. C. Verghese, and L. A. Mirny. 2007. Operating regimes of signaling cycles: statics, dynamics, and noise filtering. *PLOS Comput. Biol.* 3:e246.
- Behar, M., H. G. Dohlman, and T. C. Elston. 2007. Kinetic insulation as an effective mechanism for achieving pathway specificity in intracellular signaling networks. *Proc. Natl. Acad. Sci. USA.* 104:16146–16151.
- Kim, Y., Z. Paroush, ..., S. Y. Shvartsman. 2011. Substrate-dependent control of MAPK phosphorylation in vivo. *Mol. Syst. Biol.* 7:467.
- McClellan, M. N., A. Mody, ..., S. Ramanathan. 2007. Cross-talk and decision making in MAP kinase pathways. *Nat. Genet.* 39:409–414.
- Kim, S. Y., and J. E. Ferrell, Jr. 2007. Substrate competition as a source of ultrasensitivity in the inactivation of Wee1. *Cell.* 128:1133–1145.
- Belle, A., A. Tanay, ..., E. K. O’Shea. 2006. Quantification of protein half-lives in the budding yeast proteome. *Proc. Natl. Acad. Sci. USA.* 103:13004–13009.
- Goldbeter, A., and D. E. Koshland, Jr. 1981. An amplified sensitivity arising from covalent modification in biological systems. *Proc. Natl. Acad. Sci. USA.* 78:6840–6844.
- Bagowski, C. P., J. Besser, C. R. Frey, and J. E. Ferrell, Jr. 2003. The JNK cascade as a biochemical switch in mammalian cells: ultrasensitive and all-or-none responses. *Curr. Biol.* 13:315–320.
- Hardie, D. G., I. P. Salt, ..., S. P. Davies. 1999. AMP-activated protein kinase: an ultrasensitive system for monitoring cellular energy charge. *Biochem. J.* 338:717–722.
- Huang, C. Y., and J. E. Ferrell, Jr. 1996. Ultrasensitivity in the mitogen-activated protein kinase cascade. *Proc. Natl. Acad. Sci. USA.* 93:10078–10083.
- LaPorte, D. C., and D. E. Koshland, Jr. 1983. Phosphorylation of isocitrate dehydrogenase as a demonstration of enhanced sensitivity in covalent regulation. *Nature*. 305:286–290.
- Meinke, M. H., J. S. Bishop, and R. D. Edstrom. 1986. Zero-order ultrasensitivity in the regulation of glycogen phosphorylase. *Proc. Natl. Acad. Sci. USA.* 83:2865–2868.
- Zhang, J., P. L. Yang, and N. S. Gray. 2009. Targeting cancer with small molecule kinase inhibitors. *Nat. Rev. Cancer.* 9:28–39.
- Hindmarsh, A. C., P. N. Brown, ..., C. S. Woodward. 2005. SUNDIALS: suite of nonlinear and differential/algebraic equation solvers. *ACM Trans. Math. Software.* 31:363–396.
- Khandelwal, R. L., J. R. Vandenheede, and E. G. Krebs. 1976. Purification, properties, and substrate specificities of phosphoprotein phosphatase(s) from rabbit liver. *J. Biol. Chem.* 251:4850–4858.
- Radhakrishnan, Y., W. H. Busby, Jr., ..., D. R. Clemmons. 2010. Insulin-like growth factor-I-stimulated insulin receptor substrate-1 negatively regulates Src homology 2 domain-containing protein-tyrosine phosphatase substrate-1 function in vascular smooth muscle cells. *J. Biol. Chem.* 285:15682–15695.
- Voet, D., and J. G. Voet. 2011. Biochemistry. John Wiley & Sons, Hoboken, NJ.
- Gunawardena, J. 2005. Multisite protein phosphorylation makes a good threshold but can be a poor switch. *Proc. Natl. Acad. Sci. USA.* 102:14617–14622.
- Markevich, N. I., J. B. Hoek, and B. N. Kholodenko. 2004. Signaling switches and bistability arising from multisite phosphorylation in protein kinase cascades. *J. Cell Biol.* 164:353–359.
- Ubersax, J. A., E. L. Woodbury, ..., D. O. Morgan. 2003. Targets of the cyclin-dependent kinase Cdk1. *Nature*. 425:859–864.
- Ptacek, J., G. Devgan, ..., M. Snyder. 2005. Global analysis of protein phosphorylation in yeast. *Nature*. 438:679–684.
- Kaushansky, A., A. Gordus, ..., G. MacBeath. 2008. System-wide investigation of ErbB4 reveals 19 sites of Tyr phosphorylation that are unusually selective in their recruitment properties. *Chem. Biol.* 15:808–817.
- Hunter, T. 2007. The age of crosstalk: phosphorylation, ubiquitination, and beyond. *Mol. Cell.* 28:730–738.
- Arena, S., S. Benvenuti, and A. Bardelli. 2005. Genetic analysis of the kinome and phosphatome in cancer. *Cell. Mol. Life Sci.* 62:2092–2099.
- Manning, G., D. B. Whyte, ..., S. Sudarsanam. 2002. The protein kinase complement of the human genome. *Science*. 298:1912–1934.
- Walsh, C. 2006. Posttranslational Modification of Proteins: Expanding Nature’s Inventory. Roberts and Co. Publishers, Greenwood Village, CO.

38. Kholodenko, B. N. 2000. Negative feedback and ultrasensitivity can bring about oscillations in the mitogen-activated protein kinase cascades. *Eur. J. Biochem.* 267:1583–1588.
39. Schoeberl, B., C. Eichler-Jonsson, ..., G. Müller. 2002. Computational modeling of the dynamics of the MAP kinase cascade activated by surface and internalized EGF receptors. *Nat. Biotechnol.* 20: 370–375.
40. Shao, D., W. Zheng, ..., C. Tang. 2006. Dynamic studies of scaffold-dependent mating pathway in yeast. *Biophys. J.* 91:3986–4001.
41. Nelson, D. L., A. L. Lehninger, and M. M. Cox. 2008. *Lehninger Principles of Biochemistry*. W.H. Freeman, New York.
42. Wells, J. A., and C. L. McClendon. 2007. Reaching for high-hanging fruit in drug discovery at protein-protein interfaces. *Nature.* 450: 1001–1009.
43. Wolfram Research. 2010. *Mathematica*. Wolfram Research, Champaign, IL.
44. Loog, M., and D. O. Morgan. 2005. Cyclin specificity in the phosphorylation of cyclin-dependent kinase substrates. *Nature.* 434:104–108.
45. Yan, Z., S. A. Fedorov, ..., R. S. Williams. 2000. PR48, a novel regulatory subunit of protein phosphatase 2A, interacts with Cdc6 and modulates DNA replication in human cells. *Mol. Cell. Biol.* 20: 1021–1029.
46. Woodbury, E. L., and D. O. Morgan. 2007. Cdk and APC activities limit the spindle-stabilizing function of Fin1 to anaphase. *Nat. Cell Biol.* 9:106–112.
47. Bloom, J., I. M. Cristea, ..., F. R. Cross. 2011. Global analysis of Cdc14 phosphatase reveals diverse roles in mitotic processes. *J. Biol. Chem.* 286:5434–5445.
48. Matheos, D., M. Metodiev, ..., M. D. Rose. 2004. Pheromone-induced polarization is dependent on the Fus3p MAPK acting through the formin Bni1p. *J. Cell Biol.* 165:99–109.
49. Enserink, J. M., and R. D. Kolodner. 2010. An overview of Cdk1-controlled targets and processes. *Cell Div.* 5:11.

Crosstalk and competition in signaling networks

Supporting Material

Michael Rowland¹, Walter Fontana² and Eric J. Deeds^{1,3}

¹Center for Bioinformatics, The University of Kansas, 2030 Becker Dr., Lawrence, KS 66047, USA

²Department of Systems Biology, Harvard Medical School, 200 Longwood Avenue, Boston MA 02115, USA

³Department of Molecular Biosciences, The University of Kansas, 2030 Becker Dr., Lawrence, KS 66047, USA

Email: Michael Rowland - mrowland@ku.edu; Walter Fontana - walter@hms.harvard.edu; Eric Deeds - deeds@ku.edu;

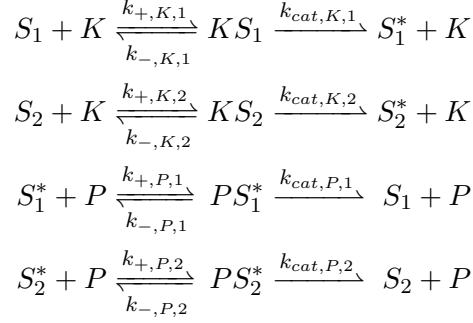
Contents

1	Systems of Ordinary Differential Equations	3
1.1	1–Kinase/1–Phosphatase Loop with 2 Substrates	3
1.2	1–Kinase/1–Phosphatase Loop with Many Substrates	4
1.3	1–Kinase/2–Phosphatase Loop	7
1.4	2–Kinase/1–Phosphatase Loop	8
1.5	Cascade with Multiple Phosphatases	10
1.6	Cascade with a Single Phosphatase	13
2	Analytical Results for the 1–Kinase/1–Phosphatase Loop	16
2.1	Mutual inhibition for competitive substrates	16
2.2	Steady-state solution for $[S_1^*]$	17
2.3	dS_1^*/dS_2^* is always positive	18
3	Analytical Results for the 1–Kinase/1–Phosphatase Loop with Many Substrates	21
4	Analytical Results for the 1–Kinase/2–Phosphatase Loop	22
4.1	$d[S_2]/d[S_2]_0$ is always positive	23
4.2	$dS_1^*/d[S_2]_0$ is always negative	24
5	Analytical Results for the 2–Kinase/1–Phosphatase Loop	25
5.1	$d[S_2^*]/d[S_2]_0$ is always positive	25
5.2	$dS_1^*/d[S_2]_0$ is always positive	26

1 Systems of Ordinary Differential Equations

1.1 1–Kinase/1–Phosphatase Loop with 2 Substrates

The set of enzymatic reactions for the 1K1P loop with two substrates is as in equation [2] of the main text:



Each contain three rates: rate of complex formation, (k_+), rate of complex dissociation (k_-), and catalytic rate (k_{cat}). The set of ODEs describing the free enzymes are:

$$\begin{aligned}
 \frac{d[K]}{dt} &= - ([S_1] \cdot [K] \cdot k_{+,K,1} + [S_2] \cdot [K] \cdot k_{+,K,2}) + ([KS_1] \cdot (k_{-,K,1} + k_{cat,K,1}) + [KS_2] \cdot (k_{-,K,2} + k_{cat,K,2})) \\
 \frac{d[P]}{dt} &= - ([S_1^*] \cdot [P] \cdot k_{+,P,1} + [S_2^*] \cdot [P] \cdot k_{+,P,2}) + ([PS_1^*] \cdot (k_{-,P,1} + k_{cat,P,1}) + [PS_2^*] \cdot (k_{-,P,2} + k_{cat,P,2}))
 \end{aligned}$$

The set of ODEs describing the unmodified substrates are:

$$\begin{aligned}
 \frac{d[S_1]}{dt} &= - ([S_1] \cdot [K] \cdot k_{+,K,1}) + ([KS_1] \cdot k_{-,K,1} + [PS_1^*] \cdot k_{cat,P,1}) \\
 \frac{d[S_2]}{dt} &= - ([S_2] \cdot [K] \cdot k_{+,K,2}) + ([KS_2] \cdot k_{-,K,2} + [PS_2^*] \cdot k_{cat,P,2})
 \end{aligned}$$

The set of ODEs describing the modified substrates are:

$$\begin{aligned}
 \frac{d[S_1^*]}{dt} &= - ([S_1^*] \cdot [P] \cdot k_{+,P,1}) + ([PS_1^*] \cdot k_{-,P,1} + [KS_1] \cdot k_{cat,K,1}) \\
 \frac{d[S_2^*]}{dt} &= - ([S_2^*] \cdot [P] \cdot k_{+,P,2}) + ([PS_2^*] \cdot k_{-,P,2} + [KS_2] \cdot k_{cat,K,2})
 \end{aligned}$$

The set of ODEs describing the enzyme-substrate complexes are:

$$\begin{aligned}
 \frac{d[KS_1]}{dt} &= - ([KS_1] \cdot (k_{-,K,1} + k_{cat,K,1})) + ([S_1] \cdot [K] \cdot k_{+,K,1}) \\
 \frac{d[KS_2]}{dt} &= - ([KS_2] \cdot (k_{-,K,2} + k_{cat,K,2})) + ([S_2] \cdot [K] \cdot k_{+,K,2}) \\
 \frac{d[PS_1^*]}{dt} &= - ([PS_1^*] \cdot (k_{-,P,1} + k_{cat,P,1})) + ([S_1^*] \cdot [P] \cdot k_{+,P,1}) \\
 \frac{d[PS_2^*]}{dt} &= - ([PS_2^*] \cdot (k_{-,P,2} + k_{cat,P,2})) + ([S_2^*] \cdot [P] \cdot k_{+,P,2})
 \end{aligned}$$

For purposes of display in Fig. 2A of the main text we used the following values for each of the rate constants:

Parameter	Value
$k_{+,K,i}$	$0.001 \text{ nM}^{-1} \cdot \text{s}^{-1}$
$k_{-,K,i}$	0.001 s^{-1}
$k_{cat,K,i}$	0.999 s^{-1}
$k_{+,P,i}$	$0.001 \text{ nM}^{-1} \cdot \text{s}^{-1}$
$k_{-,P,i}$	0.001 s^{-1}
$k_{cat,P,i}$	0.999 s^{-1}

Where $i = 1$ or 2 .

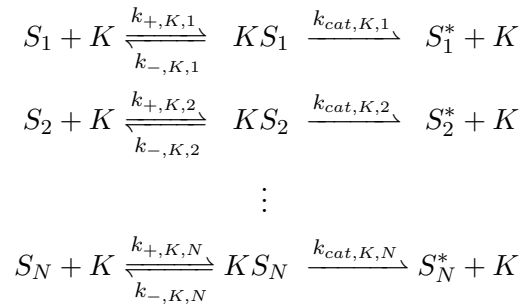
Our simulations started with the following initial concentrations:

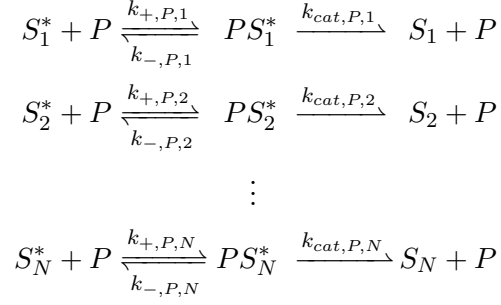
Molecular Species	Initial Concentration
K	0 - 2 nM
P	1 nM
S_1	100 nM
S_2	0 - 20 μM

With the remaining molecular species having initial concentrations of 0. The range of initial concentrations of K and S_2 were used to vary r_1 and $[S_2]_0/K_m$, respectively, in Fig. 2A in the main text.

1.2 1-Kinase/1-Phosphatase Loop with Many Substrates

The set of enzymatic reactions for the 1K1P loop with many substrates is:





The set of ODEs describing the free enzymes are:

$$\begin{aligned}
\frac{d[K]}{dt} &= - ([S_1] \cdot [K] \cdot k_{+,K,1} + [S_2] \cdot [K] \cdot k_{+,K,2} + \dots + [S_N] \cdot [K] \cdot k_{+,K,N}) \\
&\quad + ([KS_1] \cdot (k_{-,K,1} + k_{cat,K,1}) + [KS_2] \cdot (k_{-,K,2} + k_{cat,K,2}) + \dots + [KS_N] \cdot (k_{-,K,N} + k_{cat,K,N})) \\
\frac{d[P]}{dt} &= - ([S_1^*] \cdot [P] \cdot k_{+,P,1} + [S_2^*] \cdot [P] \cdot k_{+,P,2} + \dots + [S_N^*] \cdot [P] \cdot k_{+,P,N}) \\
&\quad + ([PS_1^*] \cdot (k_{-,P,1} + k_{cat,P,1}) + [PS_2^*] \cdot (k_{-,P,2} + k_{cat,P,2}) + \dots + [PS_N^*] \cdot (k_{-,P,N} + k_{cat,P,N}))
\end{aligned}$$

The set of ODEs describing the unmodified substrates are:

$$\begin{aligned}
\frac{d[S_1]}{dt} &= - ([S_1] \cdot [K] \cdot k_{+,K,1}) + ([KS_1] \cdot k_{-,K,1} + [PS_1^*] \cdot k_{cat,P,1}) \\
\frac{d[S_2]}{dt} &= - ([S_2] \cdot [K] \cdot k_{+,K,2}) + ([KS_2] \cdot k_{-,K,2} + [PS_2^*] \cdot k_{cat,P,2}) \\
&\vdots \\
\frac{d[S_N]}{dt} &= - ([S_N] \cdot [K] \cdot k_{+,K,N}) + ([KS_N] \cdot k_{-,K,N} + [PS_N^*] \cdot k_{cat,P,N})
\end{aligned}$$

The set of ODEs describing the modified substrates are:

$$\begin{aligned}
\frac{d[S_1^*]}{dt} &= - ([S_1^*] \cdot [P] \cdot k_{+,P,1}) + ([PS_1^*] \cdot k_{-,P,1} + [KS_1] \cdot k_{cat,K,1}) \\
\frac{d[S_2^*]}{dt} &= - ([S_2^*] \cdot [P] \cdot k_{+,P,2}) + ([PS_2^*] \cdot k_{-,P,2} + [KS_2] \cdot k_{cat,K,2}) \\
&\vdots \\
\frac{d[S_N^*]}{dt} &= - ([S_N^*] \cdot [P] \cdot k_{+,P,N}) + ([PS_N^*] \cdot k_{-,P,N} + [KS_N] \cdot k_{cat,K,N})
\end{aligned}$$

The set of ODEs describing the enzyme-substrate complexes are:

$$\begin{aligned}
\frac{d[KS_1]}{dt} &= - ([KS_1] \cdot (k_{-,K,1} + k_{cat,K,1})) + ([S_1] \cdot [K] \cdot k_{+,K,1}) \\
\frac{d[KS_2]}{dt} &= - ([KS_2] \cdot (k_{-,K,2} + k_{cat,K,2})) + ([S_2] \cdot [K] \cdot k_{+,K,2}) \\
&\vdots \\
\frac{d[KS_N]}{dt} &= - ([KS_N] \cdot (k_{-,K,N} + k_{cat,K,N})) + ([S_N] \cdot [K] \cdot k_{+,K,N}) \\
\frac{d[PS_1^*]}{dt} &= - ([PS_1^*] \cdot (k_{-,P,1} + k_{cat,P,1})) + ([S_1^*] \cdot [P] \cdot k_{+,P,1}) \\
\frac{d[PS_2^*]}{dt} &= - ([PS_2^*] \cdot (k_{-,P,2} + k_{cat,P,2})) + ([S_2^*] \cdot [P] \cdot k_{+,P,2}) \\
&\vdots \\
\frac{d[PS_N^*]}{dt} &= - ([PS_N^*] \cdot (k_{-,P,N} + k_{cat,P,N})) + ([S_N^*] \cdot [P] \cdot k_{+,P,N})
\end{aligned}$$

The following values for rate constants were used in the simulations presented in Fig. 2B of the main text:

Parameter	Value
$k_{+,K,i}$	$0.001 \text{ nM}^{-1} \cdot \text{s}^{-1}$
$k_{-,K,i}$	0.001 s^{-1}
$k_{cat,K,i}$	0.999 s^{-1}
$k_{+,P,i}$	$0.001 \text{ nM}^{-1} \cdot \text{s}^{-1}$
$k_{-,P,i}$	0.001 s^{-1}
$k_{cat,P,i}$	0.999 s^{-1}

The different molecular species were initialized with concentrations:

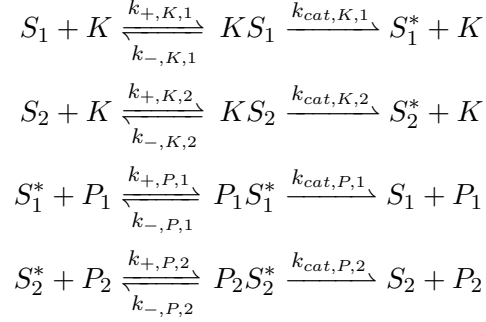
Molecular Species	Initial Concentration
K	0 - 2 nM
P	1 nM
S_i	500 nM

$$i = 1, 2, \dots, N$$

The remaining molecular species had initial concentrations of 0. The range of initial concentrations of K was used to vary the value of r_1 , and N was varied to obtain the surface in Fig. 2B in the main text.

1.3 1–Kinase/2–Phosphatase Loop

The set of enzymatic reactions for the 1K2P loop is:



The set of ODEs describing the free enzymes are:

$$\begin{aligned}
 \frac{d[K]}{dt} &= - ([S_1] \cdot [K] \cdot k_{+,K,1} + [S_2] \cdot [K] \cdot k_{+,K,2}) + ([KS_1] \cdot (k_{-,K,1} + k_{cat,K,1}) + [KS_2] \cdot (k_{-,K,2} + k_{cat,K,2})) \\
 \frac{d[P_1]}{dt} &= - ([S_1^*] \cdot [P_1] \cdot k_{+,P,1}) + ([P_1S_1^*] \cdot (k_{-,P,1} + k_{cat,P,1})) \\
 \frac{d[P_2]}{dt} &= - ([S_2^*] \cdot [P_2] \cdot k_{+,P,2}) + ([P_2S_2^*] \cdot (k_{-,P,2} + k_{cat,P,2}))
 \end{aligned}$$

The set of ODEs describing the unmodified substrates are:

$$\begin{aligned}
 \frac{d[S_1]}{dt} &= - ([S_1] \cdot [K] \cdot k_{+,K,1}) + ([KS_1] \cdot k_{-,K,1} + [P_1S_1^*] \cdot k_{cat,P,1}) \\
 \frac{d[S_2]}{dt} &= - ([S_2] \cdot [K] \cdot k_{+,K,2}) + ([KS_2] \cdot k_{-,K,2} + [P_2S_2^*] \cdot k_{cat,P,2})
 \end{aligned}$$

The set of ODEs describing the modified substrates are:

$$\begin{aligned}
 \frac{d[S_1^*]}{dt} &= - ([S_1^*] \cdot [P_1] \cdot k_{+,P,1}) + ([P_1S_1^*] \cdot k_{-,P,1} + [KS_1] \cdot k_{cat,K,1}) \\
 \frac{d[S_2^*]}{dt} &= - ([S_2^*] \cdot [P_2] \cdot k_{+,P,2}) + ([P_2S_2^*] \cdot k_{-,P,2} + [KS_2] \cdot k_{cat,K,2})
 \end{aligned}$$

The set of ODEs describing the enzyme-substrate complexes are:

$$\begin{aligned}
 \frac{d[KS_1]}{dt} &= - ([KS_1] \cdot (k_{-,K,1} + k_{cat,K,1})) + ([S_1] \cdot [K] \cdot k_{+,K,1}) \\
 \frac{d[KS_2]}{dt} &= - ([KS_2] \cdot (k_{-,K,2} + k_{cat,K,2})) + ([S_2] \cdot [K] \cdot k_{+,K,2}) \\
 \frac{d[P_1S_1^*]}{dt} &= - ([P_1S_1^*] \cdot (k_{-,P,1} + k_{cat,P,1})) + ([S_1^*] \cdot [P_1] \cdot k_{+,P,1}) \\
 \frac{d[P_2S_2^*]}{dt} &= - ([P_2S_2^*] \cdot (k_{-,P,2} + k_{cat,P,2})) + ([S_2^*] \cdot [P_2] \cdot k_{+,P,2})
 \end{aligned}$$

For purposes of display in Figs. 3A and B in the main text, we used the following parameters in the model:

Parameter	Value
$k_{+,K,i}$	$0.001 \text{ nM}^{-1} \cdot \text{s}^{-1}$
$k_{-,K,i}$	0.001 s^{-1}
$k_{cat,K,i}$	0.999 s^{-1}
$k_{+,P,i}$	$0.001 \text{ nM}^{-1} \cdot \text{s}^{-1}$
$k_{-,P,i}$	0.001 s^{-1}
$k_{cat,P,i}$	0.999 s^{-1}

$i = 1 \text{ or } 2$

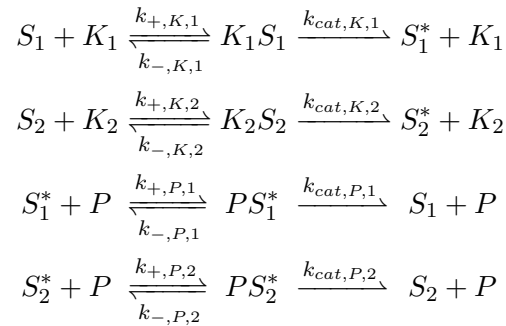
Each of the molecular species in the model started with the following initial concentrations:

Molecular Species	Initial Concentration
K	1 nM
P_1	0.5-100 nM
P_2	0.5-100 nM
S_1	100 nM
S_2	0, 20 μM

The remaining molecular species had initial concentrations of 0. The range of initial concentrations for P_1 and P_2 were used to independently set r_1 and r_2 , respectively, in Figs. 3A and B in the main text. In Fig. 3A $[S_2]_0 = 0$ and in Fig 3B $[S_2]_0 = 20 \text{ nM}$.

1.4 2-Kinase/1-Phosphatase Loop

The set of enzymatic reactions for the 2K1P loop is:



The set of ODEs describing the free enzymes are:

$$\begin{aligned}\frac{d[K_1]}{dt} &= - ([S_1] \cdot [K_1] \cdot k_{+,K,1}) + ([K_1S_1] \cdot (k_{-,K,1} + k_{cat,K,1})) \\ \frac{d[K_2]}{dt} &= - ([S_2] \cdot [K_2] \cdot k_{+,K,2}) + ([K_2S_2] \cdot (k_{-,K,2} + k_{cat,K,2})) \\ \frac{d[P]}{dt} &= - ([S_1^*] \cdot [P] \cdot k_{+,P,1} + [S_2^*] \cdot [P] \cdot k_{+,P,2}) + ([PS_1^*] \cdot (k_{-,P,1} + k_{cat,P,1}) + [PS_2^*] \cdot (k_{-,P,2} + k_{cat,P,2}))\end{aligned}$$

The set of ODEs describing the unmodified substrates are:

$$\begin{aligned}\frac{d[S_1]}{dt} &= - ([S_1] \cdot [K_1] \cdot k_{+,K,1}) + ([K_1S_1] \cdot k_{-,K,1} + [PS_1^*] \cdot k_{cat,P,1}) \\ \frac{d[S_2]}{dt} &= - ([S_2] \cdot [K_2] \cdot k_{+,K,2}) + ([K_2S_2] \cdot k_{-,K,2} + [PS_2^*] \cdot k_{cat,P,2})\end{aligned}$$

The set of ODEs describing the modified substrates are:

$$\begin{aligned}\frac{d[S_1^*]}{dt} &= - ([S_1^*] \cdot [P] \cdot k_{+,P,1}) + ([PS_1^*] \cdot k_{-,P,1} + [K_1S_1] \cdot k_{cat,K,1}) \\ \frac{d[S_2^*]}{dt} &= - ([S_2^*] \cdot [P] \cdot k_{+,P,2}) + ([PS_2^*] \cdot k_{-,P,2} + [K_2S_2] \cdot k_{cat,K,2})\end{aligned}$$

The set of ODEs describing the enzyme-substrate complexes are:

$$\begin{aligned}\frac{d[K_1S_1]}{dt} &= - ([K_1S_1] \cdot (k_{-,K,1} + k_{cat,K,1})) + ([S_1] \cdot [K_1] \cdot k_{+,K,1}) \\ \frac{d[K_2S_2]}{dt} &= - ([K_2S_2] \cdot (k_{-,K,2} + k_{cat,K,2})) + ([S_2] \cdot [K_2] \cdot k_{+,K,2}) \\ \frac{d[PS_1^*]}{dt} &= - ([PS_1^*] \cdot (k_{-,P,1} + k_{cat,P,1})) + ([S_1^*] \cdot [P] \cdot k_{+,P,1}) \\ \frac{d[PS_2^*]}{dt} &= - ([PS_2^*] \cdot (k_{-,P,2} + k_{cat,P,2})) + ([S_2^*] \cdot [P] \cdot k_{+,P,2})\end{aligned}$$

For purposes of display in Figs. 3A and C in the main text we used the following parameters:

Parameter	Value
$k_{+,K,i}$	$0.001 \text{ nM}^{-1} \cdot \text{s}^{-1}$
$k_{-,K,i}$	0.001 s^{-1}
$k_{cat,K,i}$	0.999 s^{-1}
$k_{+,P,i}$	$0.001 \text{ nM}^{-1} \cdot \text{s}^{-1}$
$k_{-,P,i}$	0.001 s^{-1}
$k_{cat,P,i}$	0.999 s^{-1}

$i = 1 \text{ or } 2$

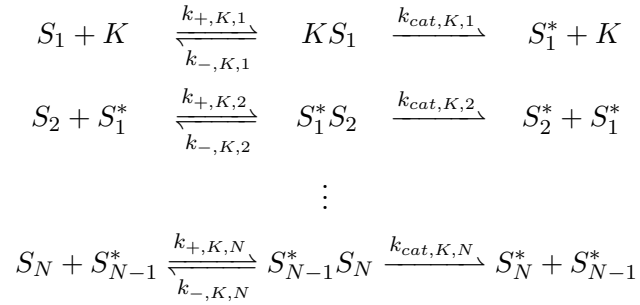
Each molecular species were initialized at the following concentrations:

Molecular Species	Initial Concentration
K_1	0 - 2 nM
K_2	0 - 2 nM
P	1 nM
S_1	100 nM
S_2	0, 20 μ M

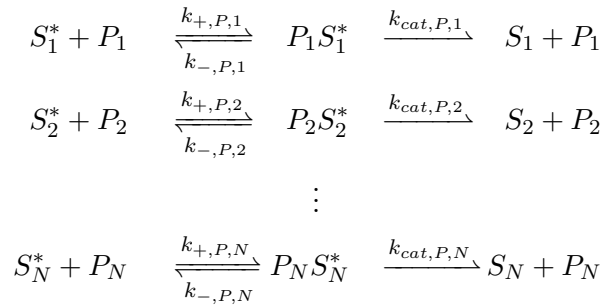
The remaining molecular species had initial concentrations of 0. The range of initial concentrations of K_1 and K_2 were used to set the values of r_1 and r_2 , respectively, in Figs. 3A and C in the main text. In Fig. 3A, $[S_2]_0 = 0$ and in Fig. 3C, $[S_2]_0 = 20nM$.

1.5 Cascade with Multiple Phosphatases

The set of kinase enzymatic reactions for the cascade with multiple phosphatases is:



Note that K is the input kinase and S_i^* serves as the kinase for S_{i+1} . The set of phosphatase enzymatic reactions is:



The set of ODEs describing the free enzymes are:

$$\begin{aligned}
\frac{d[K]}{dt} &= - ([S_1] \cdot [K] \cdot k_{+,K,1}) + ([KS_1] \cdot (k_{-,K,1} + k_{cat,K,1})) \\
\frac{d[P_1]}{dt} &= - ([S_1^*] \cdot [P_1] \cdot k_{+,P,1}) + ([P_1S_1^*] \cdot (k_{-,P,1} + k_{cat,P,1})) \\
\frac{d[P_i]}{dt} &= - ([S_i^*] \cdot [P_i] \cdot k_{+,P,i}) + ([P_iS_i^*] \cdot (k_{-,P,i} + k_{cat,P,i})) \\
\frac{d[P_N]}{dt} &= - ([S_N^*] \cdot [P_N] \cdot k_{+,P,N}) + ([P_NS_N^*] \cdot (k_{-,P,N} + k_{cat,P,N}))
\end{aligned}$$

The set of ODEs describing the unmodified substrates are:

$$\begin{aligned}
\frac{d[S_1]}{dt} &= - ([S_1] \cdot [K] \cdot k_{+,K,1}) + ([KS_1] \cdot k_{-,K,1} + [P_1S_1^*] \cdot k_{cat,P,1}) \\
\frac{d[S_i]}{dt} &= - ([S_i] \cdot [S_{i-1}^*] \cdot k_{+,K,i}) + ([S_{i-1}^*S_i] \cdot k_{-,K,i} + [P_iS_i^*] \cdot k_{cat,P,i}) \\
\frac{d[S_N]}{dt} &= - ([S_N] \cdot [S_{N-1}^*] \cdot k_{+,K,N}) + ([S_{N-1}^*S_N] \cdot k_{-,K,N} + [P_NS_N^*] \cdot k_{cat,P,N})
\end{aligned}$$

The set of ODEs describing the modified substrates are:

$$\begin{aligned}
\frac{d[S_1^*]}{dt} &= - ([S_1^*] \cdot [P] \cdot k_{+,K,1}) + [S_2] \cdot [S_1^*] \cdot k_{+,K,2} \\
&\quad + ([P_1S_1^*] \cdot k_{-,P,1} + [KS_1] \cdot k_{cat,K,1} + [S_1^*S_2] \cdot (k_{-,K,2} + k_{cat,K,2})) \\
\frac{d[S_i^*]}{dt} &= - ([S_i^*] \cdot [P_i] \cdot k_{+,K,i}) + [S_{i+1}] \cdot [S_i^*] \cdot k_{+,K,i+1} \\
&\quad + ([P_iS_i^*] \cdot k_{-,P,i} + [S_{i-1}^*S_i] \cdot k_{cat,K,i} + [S_i^*S_{i+1}] \cdot (k_{-,K,i+1} + k_{cat,K,i+1})) \\
\frac{d[S_N^*]}{dt} &= - ([S_N^*] \cdot [P_N] \cdot k_{+,K,N}) + ([P_NS_N^*] \cdot k_{-,P,N} + [S_{N-1}^*S_N] \cdot k_{cat,K,N})
\end{aligned}$$

The set of ODEs describing the enzyme-substrate complexes are:

$$\begin{aligned}
\frac{d[KS_1]}{dt} &= - ([KS_1] \cdot (k_{-,K,1} + k_{cat,K,1})) + ([S_1] \cdot [K] \cdot k_{+,K,1}) \\
\frac{d[S_{i-1}^*S_i]}{dt} &= - ([S_{i-1}^*S_i] \cdot (k_{-,K,i} + k_{cat,K,i})) + ([S_i] \cdot [S_{i-1}^*] \cdot k_{+,K,i}) \\
\frac{d[S_{N-1}^*S_N]}{dt} &= - ([S_{N-1}^*S_N] \cdot (k_{-,K,N} + k_{cat,K,N})) + ([S_N] \cdot [S_{N-1}^*] \cdot k_{+,K,N}) \\
\frac{d[P_1S_1^*]}{dt} &= - ([P_1S_1^*] \cdot (k_{-,P,1} + k_{cat,P,1})) + ([S_1^*] \cdot [P_1] \cdot k_{+,P,1}) \\
\frac{d[P_iS_i^*]}{dt} &= - ([P_iS_i^*] \cdot (k_{-,P,i} + k_{cat,P,i})) + ([S_i^*] \cdot [P_i] \cdot k_{+,P,i}) \\
\frac{d[P_NS_N^*]}{dt} &= - ([P_NS_N^*] \cdot (k_{-,P,N} + k_{cat,P,N})) + ([S_N^*] \cdot [P_N] \cdot k_{+,P,N})
\end{aligned}$$

Where $i = 2, \dots, N - 1$.

For purposes of display in Fig. 3D in the main text, we used the following parameters:

Parameter	Value
$k_{+,K,i}$	$0.001 \text{ nM}^{-1} \cdot \text{s}^{-1}$
$k_{-,K,i}$	10^{i-8} s^{-1}
$k_{cat,K,i}$	$0.999 \cdot 10^{i-5} \text{ s}^{-1}$
$k_{+,P,i}$	$0.001 \text{ nM}^{-1} \cdot \text{s}^{-1}$
$k_{-,P,i}$	10^{i-8} s^{-1}
$k_{cat,P,i}$	$0.999 \cdot 10^{i-5} \text{ s}^{-1}$

$$i = 1, 2, \dots, N$$

The k_{cat} 's and k_- 's were calculated as $0.999 \cdot 10^{i-5} \text{ s}^{-1}$ and 10^{i-8} s^{-1} , respectively; the kinetic parameters of reaction i in the cascade were thus varied so that each substrate concentration was $10 \cdot K_m$ in respect to its kinase and phosphatase.

The molecular species in the system started with the following initial concentrations:

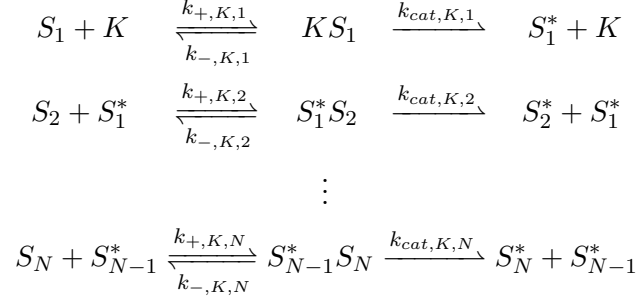
Molecular Species	Initial Concentration
K	$10^{-18} - 0.1 \text{ nM}$
P_i	0.01 nM
S_1	1 nM
S_2	10 nM
\vdots	\vdots
S_i	$10 \cdot S_{i-1}$
\vdots	\vdots
S_N	$10 \cdot S_{N-1}$

$$i = 1, 2, \dots, N$$

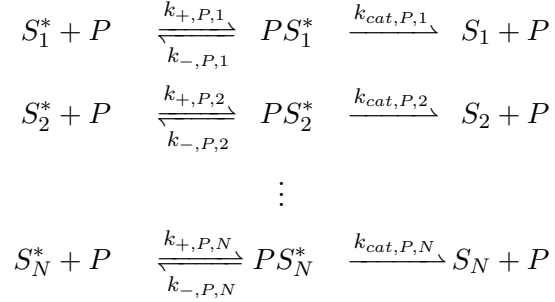
The remaining molecular species had initial concentrations of 0. We systematically increased the initial concentration of the S_i 's ($[S_i]_0 = 10 \cdot [S_{i-1}]_0$); since S_{i-1}^* is the kinase for S_i , this ensured that all substrates were at higher concentrations than their enzymes. The range of initial concentrations of K were used to vary the value of r in Fig. 3D.

1.6 Cascade with a Single Phosphatase

The set of kinase enzymatic reactions for the cascade with a single phosphatase is:



The set of phosphatase enzymatic reactions is:



The set of ODEs describing free enzymes are:

$$\begin{aligned}
 \frac{d[K]}{dt} &= - ([S_1] \cdot [K] \cdot k_{+,K,1}) + ([KS_1] \cdot (k_{-,K,1} + k_{cat,K,1})) \\
 \frac{d[P]}{dt} &= - ([S_1^*] \cdot [P] \cdot k_{+,P,1} + [S_2^*] \cdot k_{+,P,2} + \dots + [S_N^*] \cdot k_{+,P,N}) \\
 &\quad + ([PS_1^*] \cdot (k_{-,P,1} + k_{cat,P,1}) + [PS_2^*] \cdot (k_{-,P,2} + k_{cat,P,2}) + \dots + [PS_N^*] \cdot (k_{-,P,N} + k_{cat,P,N}))
 \end{aligned}$$

The set of ODEs describing unmodified substrates are:

$$\begin{aligned}
 \frac{d[S_1]}{dt} &= - ([S_1] \cdot [K] \cdot k_{+,K,1}) + ([KS_1] \cdot k_{-,K,1} + [PS_1^*] \cdot k_{cat,P,1}) \\
 \frac{d[S_i]}{dt} &= - ([S_i] \cdot [S_{i-1}^*] \cdot k_{+,K,i}) + ([S_{i-1}^* S_i] \cdot k_{-,K,i} + [PS_i^*] \cdot k_{cat,P,i}) \\
 \frac{d[S_N]}{dt} &= - ([S_N] \cdot [S_{N-1}^*] \cdot k_{+,K,N}) + ([S_{N-1}^* S_N] \cdot k_{-,K,N} + [PS_N^*] \cdot k_{cat,P,N})
 \end{aligned}$$

The set of ODEs describing modified substrates are:

$$\begin{aligned}
\frac{d[S_1^*]}{dt} &= - ([S_1^*] \cdot [P] \cdot k_{+,K,1}) + [S_2] \cdot [S_1^*] * k_{+,K,2}) \\
&\quad + ([PS_1^*] \cdot k_{-,P,1} + [KS_1] \cdot k_{cat,K,1} + [S_1^*S_2] \cdot (k_{-,K,2} + k_{cat,K,2})) \\
\frac{d[S_i^*]}{dt} &= - ([S_i^*] \cdot [P] \cdot k_{+,K,i}) + [S_{i+1}] \cdot [S_i^*] * k_{+,K,i+1}) \\
&\quad + ([PS_i^*] \cdot k_{-,P,i} + [S_{i-1}^*S_i] \cdot k_{cat,K,i} + [S_i^*S_{i+1}] \cdot (k_{-,K,i+1} + k_{cat,K,i+1})) \\
\frac{d[S_N^*]}{dt} &= - ([S_N^*] \cdot [P] \cdot k_{+,K,N}) + ([PS_N^*] \cdot k_{-,P,N} + [S_{N-1}^*S_N] \cdot k_{cat,K,N})
\end{aligned}$$

The set of ODEs describing enzyme-substrate complexes are:

$$\begin{aligned}
\frac{d[KS_1]}{dt} &= - ([KS_1] \cdot (k_{-,K,1} + k_{cat,K,1})) + ([S_1] \cdot [K] \cdot k_{+,K,1}) \\
\frac{d[PS_1^*]}{dt} &= - ([PS_1^*] \cdot (k_{-,P,1} + k_{cat,P,1})) + ([S_1^*] \cdot [P] \cdot k_{+,P,1}) \\
\frac{d[S_{i-1}^*S_i]}{dt} &= - ([S_{i-1}^*S_i] \cdot (k_{-,K,i} + k_{cat,K,i})) + ([S_i] \cdot [S_{i-1}^*] \cdot k_{+,K,i}) \\
\frac{d[PS_i^*]}{dt} &= - ([PS_i^*] \cdot (k_{-,P,i} + k_{cat,P,i})) + ([S_i^*] \cdot [P] \cdot k_{+,P,i}) \\
\frac{d[S_{N-1}^*S_N]}{dt} &= - ([S_{N-1}^*S_N] \cdot (k_{-,K,N} + k_{cat,K,N})) + ([S_N] \cdot [S_{N-1}^*] \cdot k_{+,K,N}) \\
\frac{d[P_N S_N^*]}{dt} &= - ([P_N S_N^*] \cdot (k_{-,P,N} + k_{cat,P,N})) + ([S_N^*] \cdot [P] \cdot k_{+,P,N})
\end{aligned}$$

Where $i = 2, \dots, N - 1$.

For purposes of display in Fig. 3D, we used the following parameters:

Parameter	Value
$k_{+,K,i}$	$0.001 \text{ nM}^{-1} \cdot \text{s}^{-1}$
$k_{-,K,i}$	$(10^{i-8}) \text{ s}^{-1}$
$k_{cat,K,i}$	$(0.999 \cdot 10^{i-5}) \text{ s}^{-1}$
$k_{+,P,i}$	$0.001 \text{ nM}^{-1} \cdot \text{s}^{-1}$
$k_{-,P,i}$	$(10^{i-8}) \text{ s}^{-1}$
$k_{cat,P,i}$	$(0.999 \cdot 10^{i-5}) \text{ s}^{-1}$

The k_{cat} 's and k_- 's were calculated as in section 1.5.

The molecular species were initialized at the following concentrations:

Molecular Species	Initial Concentration
K	10^{-18} - 0.1 nM
P	0.01 nM
S_1	1 nM
S_2	10 nM
\vdots	\vdots
S_i	$10 \cdot S_{i-1}$
\vdots	\vdots
S_N	$10 \cdot S_{N-1}$

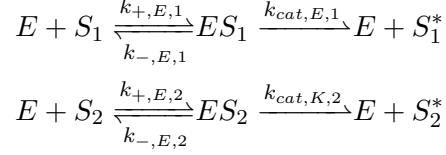
$$i = 1, 2, \dots, N$$

Remaining molecular species were set with initial concentrations of 0. Increasing the initial concentrations of S_i ensured that $[S_i]_0 = 10 \cdot [S_{i-1}]_0$ since S_{i-1}^* is the kinase for S_i to ensure that the concentration of substrates were larger than the concentrations of their respective kinases. The range of initial concentrations of K were used to vary the value of r in Fig. 3D.

2 Analytical Results for the 1–Kinase/1–Phosphatase Loop

2.1 Mutual inhibition for competitive substrates

Here we will show that the 1K1P loop displays behavior dependent on r without regard for other parameters. The enzymatic reactions for an enzyme with two substrates can be written as:



with $E = K$ or P . The Michaelis-Menten constant and maximum velocity of the enzyme for either substrate are defined as:

$$\begin{aligned} K_{m,E,x} &\equiv \frac{k_{-,E,x} + k_{cat,E,x}}{k_{+,E,x}} \\ V_{max,E,x} &\equiv k_{cat,E,x}[E]_0 \end{aligned}$$

We can obtain the following kinetic equations:

$$\frac{d[ES_1]}{dt} = [E][S_1]k_{+,E,1} - [ES_1](k_{-,E,1} + k_{cat,E,1}) \quad (2.1.1)$$

$$\frac{d[ES_2]}{dt} = [E][S_2]k_{+,E,2} - [ES_2](k_{-,E,2} + k_{cat,E,2}) \quad (2.1.2)$$

$$\frac{d[S_1^*]}{dt} = k_{cat,E,1}[ES_1] \quad (2.1.3)$$

We also have the conservation of mass:

$$[E]_0 = [E] + [ES_1] + [ES_2] \quad (2.1.4)$$

Assuming pseudo-steady state for the enzymatic reactions, from equations 2.1.1 and 2.1.2 we get:

$$[ES_1] = \frac{[E][S_1]}{K_{m,E,1}}$$

$$[ES_2] = \frac{[E][S_2]}{K_{m,E,2}}$$

both of which can be substituted into equation 2.1.4:

$$\begin{aligned} [E]_0 &= [E] \left(1 + \frac{[S_1]}{K_{m,E,1}} + \frac{[S_2]}{K_{m,E,2}} \right) \\ [E] &= \frac{[E]_0}{1 + \frac{[S_1]}{K_{m,E,1}} + \frac{[S_2]}{K_{m,E,2}}} \end{aligned}$$

$$[ES_1] = \frac{[E]_0[S_1]}{[S_1] + K_{m,E,1} \left(1 + \frac{[S_2]}{K_{m,E,2}}\right)}$$

This can be substituted into 2.1.3 to arrive at:

$$\begin{aligned} \frac{d[S_1^*]}{dt} &= \frac{V_{max,E,1}[S_1]}{\alpha_{E,1}K_{m,E,1} + [S_1]} \\ \alpha_{E,1} &\equiv 1 + \frac{[S_2]}{K_{m,E,2}} \end{aligned} \quad (2.1.5)$$

where $\alpha_{E,1}$ is the inhibitory constant for S_2 competition with S_1 for E .

2.2 Steady-state solution for $[S_1^*]$

As Goldbeter and Koshland originally noted, for a futile cycle at steady state we will have $d[S_1^*]/dt = d[S_1]/dt$ [1]. Given 2.1.5, for the 1K1P loop with two substrates this yields:

$$\frac{V_{max,K,1}[S_1]}{\alpha_{K,1}K_{m,K,1} + [S_1]} = \frac{V_{max,P,1}[S_1^*]}{\alpha_{P,1}K_{m,P,1} + [S_1^*]} \quad (2.2.1)$$

Following the standard Michaelis-Menten assumptions [1, 2], we have that $[S_i]_0 \gg [K]_0, [P]_0$. This gives us $[S_1]_0 = [S_1] + [S_1^*]$, which can be substituted into 2.2.1:

$$\frac{V_{max,K,1}([S_1]_0 - [S_1^*])}{\alpha_{K,1}K_{m,K,1} + ([S_1]_0 - [S_1^*])} = \frac{V_{max,P,1}[S_1^*]}{\alpha_{P,1}K_{m,P,1} + [S_1^*]}$$

Dividing both sides by $[S_1]_0$, we get:

$$\frac{V_{max,K,1}(1 - S_1^*)}{\alpha_{K,1}K_{K,1} + (1 - S_1^*)} = \frac{V_{max,P,1}S_1^*}{\alpha_{P,1}K_{P,1} + S_1^*} \quad (2.2.2)$$

$$\begin{aligned} K_{K,1} &\equiv \frac{K_{m,K,1}}{[S_1]_0}, \quad K_{P,1} \equiv \frac{K_{m,P,1}}{[S_1]_0} \\ S_1 &\equiv \frac{[S_1]}{[S_1]_0}, \quad S_1^* \equiv \frac{[S_1^*]}{[S_1]_0} \end{aligned}$$

We can expand 2.2.2:

$$\begin{aligned} \alpha_{P,1}V_{max,K,1}K_{P,1} - \alpha_{P,1}V_{max,K,1}K_{P,1}S_1^* + V_{max,K,1}S_1^* - V_{max,K,1}(S_1^*)^2 \\ = \alpha_{K,1}V_{max,P,1}K_{K,1}S_1^* + V_{max,P,1}S_1^* - V_{max,P,1}(S_1^*)^2 \end{aligned}$$

Dividing both sides by $V_{max,P,1}$, we get:

$$r_1\alpha_{P,1}K_{P,1} - r_1\alpha_{P,1}K_{P,1}S_1^* + r_1S_1^* - r_1(S_1^*)^2 = \alpha_{K,1}K_{K,1}S_1^* + S_1^* - (S_1^*)^2$$

$$r_1 \equiv \frac{V_{max,K,1}}{V_{max,P,1}}$$

which can be simplified to:

$$(1 - r_1)(S_1^*)^2 + ((r_1 - 1) - (\alpha_{K,1}K_{K,1} + r_1\alpha_{P,1}K_{P,1}))S_1^* + r_1\alpha_{P,1}K_{P,1} = 0 \quad (2.2.3)$$

Solving for S_1^* :

$$S_1^* = \frac{(r_1 - 1) - (\alpha_{K,1}K_{K,1} + r_1\alpha_{P,1}K_{P,1}) + \sqrt{((r_1 - 1) - (\alpha_{K,1}K_{K,1} + r_1\alpha_{P,1}K_{P,1}))^2 + 4(r_1 - 1)r_1\alpha_{P,1}K_{P,1}}}{2(r_1 - 1)} \quad (2.2.4)$$

There are two important things to note about this solution. For one, the above equation is valid for $r_1 > 0$; at $r_1 = 0$ one needs to take the other branch of the solution (i.e. the branch in which the square root term is subtracted in the numerator). Also, at $r_1 = 1$, 2.2.4 has a nonessential singularity. To obtain the behavior at $r_1 = 1$, we see 2.2.3 becomes:

$$-(\alpha_{K,1}K_{K,1} + \alpha_{P,1}K_{P,1})S_1^* + \alpha_{P,1}K_{P,1} = 0 \quad (2.2.5)$$

giving us S_1^* for $r_1 = 1$:

$$S_1^* = \frac{\alpha_{P,1}K_{P,1}}{\alpha_{K,1}K_{K,1} + \alpha_{P,1}K_{P,1}} \quad (2.2.6)$$

2.3 dS_1^*/dS_2^* is always positive

We wish to show that $\frac{dS_1^*}{dS_2^*} > 0$ regardless of the values of any parameter. This would indicate that the ultrasensitivity of S_2 transfers to S_1 (i.e., since S_2^* will decrease as $[S_2]_0$ increases for $r_2 < 1$, S_1^* would also decrease). To do so we notice that, by the chain rule:

$$\frac{dS_1^*}{dS_2^*} = \frac{\partial S_1^*}{\partial \alpha_{K,1}} \cdot \frac{d\alpha_{K,1}}{dS_2^*} + \frac{\partial S_1^*}{\partial \alpha_{P,1}} \cdot \frac{d\alpha_{P,1}}{dS_2^*} \quad (2.3.1)$$

This is because S_1^* is a function of $\alpha_{K,1}$, $\alpha_{P,1}$, r_1 , and a vector of positive constants 2.2.4. Each of the α terms are, in turn, functions of S_2^* .

We will explore the signs of each component of 2.3.1 to show that $\frac{dS_1^*}{dS_2^*} > 0$. Using

Mathematica [3], we can obtain the partial derivative of 2.2.4 with respect to $\alpha_{K,1}$ at $r_1 \neq 1$:

$$\frac{\partial S_1^*}{\partial \alpha_{K,1}} = \frac{-K_{K,1} + \frac{K_{K,1}x}{\sqrt{x^2+y}}}{2(r_1 - 1)} \quad (2.3.2)$$

Where:

$$x \equiv -((r_1 - 1) - (\alpha_{K,1}K_{K,1} + r_1\alpha_{P,1}K_{P,1})), \quad y \equiv 4(r_1 - 1)r_1\alpha_{P,1}K_{P,1} \quad (2.3.3)$$

Factoring out $\frac{-K_{K,1}}{\sqrt{x^2+y}}$ we obtain:

$$\frac{\partial S_1^*}{\partial \alpha_{K,1}} = \frac{-K_{K,1}}{\sqrt{x^2+y}} \cdot \frac{-x + \sqrt{x^2+y}}{2(r_1 - 1)} \quad (2.3.4)$$

Notice that the second term in 2.3.4 is the expression for S_1^* , simplifying $\frac{dS_1^*}{d\alpha_{K,1}}$ to:

$$\frac{\partial S_1^*}{\partial \alpha_{K,1}} = \frac{-K_{K,1}}{\sqrt{x^2+y}} S_1^* \quad (2.3.5)$$

Note that $K_{K,1}$, S_1^* and $\sqrt{x^2+y}$ are all positive, making $\frac{\partial S_1^*}{\partial \alpha_{K,1}} < 0$ for $r_1 \neq 1$. We can also demonstrate this for $r_1 = 1$ by taking the partial derivative of 2.2.6 with respect to $\alpha_{K,1}$:

$$\frac{\partial S_1^*}{\partial \alpha_{K,1}} = \frac{-\alpha_{P,1}K_{K,1}K_{P,1}}{(\alpha_{K,1}K_{K,1} + \alpha_{P,1}K_{P,1})^2} \quad (2.3.6)$$

Which is clearly negative, demonstrating that $\frac{\partial S_1^*}{\partial \alpha_{K,1}} < 0$ for any set of parameters.

Next it can be shown that $\frac{\partial S_1^*}{\partial \alpha_{P,1}} > 0$. We can obtain an expression the partial derivative of 2.2.4 with respect to $\alpha_{P,1}$ at $r_1 \neq 1$ with Mathematica [3] :

$$\frac{\partial S_1^*}{\partial \alpha_{P,1}} = \frac{-r_1K_{P,1} + \frac{2(r_1-1)r_1K_{P,1} + r_1K_{P,1}x}{\sqrt{x^2+y}}}{2(r_1 - 1)} \quad (2.3.7)$$

By factoring out $\frac{r_1K_{P,1}}{\sqrt{x^2+y}}$ we get:

$$\frac{\partial S_1^*}{\partial \alpha_{P,1}} = \frac{r_1K_{P,1}}{\sqrt{x^2+y}} \left(\frac{2(r_1 - 1) + x - \sqrt{x^2+y}}{2(r_1 - 1)} \right) \quad (2.3.8)$$

Notice that the second term in 2.3.8 is the expression for $1 - S_1^*$, simplifying $\frac{\partial S_1^*}{\partial \alpha_{P,1}}$ to:

$$\frac{\partial S_1^*}{\partial \alpha_{P,1}} = \frac{r_1K_{P,1}}{\sqrt{x^2+y}} (1 - S_1^*) \quad (2.3.9)$$

We can easily see that 2.3.9 is positive, confirming $\frac{\partial S_1^*}{\partial \alpha_{P,1}} > 0$ for $r_1 \neq 1$. We can also demonstrate this for $r_1 = 1$ by taking the partial derivative of 2.2.6 with respect to $\alpha_{P,1}$:

$$\frac{\partial S_1^*}{\partial \alpha_{P,1}} = \frac{\alpha_{K,1} K_{K,1} K_{P,1}}{(\alpha_{K,1} K_{K,1} + \alpha_{P,1} K_{P,1})^2} \quad (2.3.10)$$

Which is clearly positive, demonstrating that $\frac{\partial S_1^*}{\partial \alpha_{P,1}} > 0$ for any set of parameters.

It is easy to show that $\frac{d\alpha_{K,1}}{dS_2^*} < 0$:

$$\begin{aligned} \alpha_{K,1} &= 1 + \frac{[S_2]}{K_{m,K,2}} \\ &= 1 + \frac{[S_2]_0 - [S_2^*]}{K_{m,K,2}} \\ &= 1 + \frac{1 - S_2^*}{K_{K,2}} \\ \frac{d\alpha_{K,1}}{dS_2^*} &= -\frac{1}{K_{K,2}} < 0 \end{aligned}$$

Similarly, we can show $\frac{d\alpha_{P,1}}{dS_2^*} > 0$:

$$\begin{aligned} \alpha_{P,1} &= 1 + \frac{[S_2^*]}{K_{m,P,2}} \\ &= 1 + \frac{S_2^*}{K_{P,2}} \\ \frac{d\alpha_{P,1}}{dS_2^*} &= \frac{1}{K_{P,2}} > 0 \end{aligned}$$

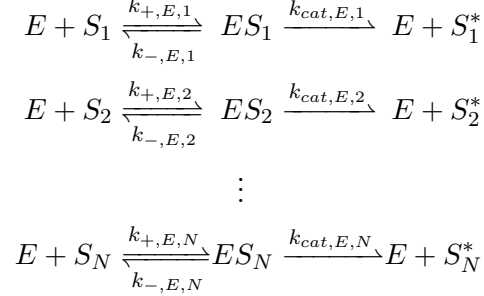
Now we have determined the behaviors of each component of the two implementations of the chain rules presented in 2.3.1 for all values of r_1 and r_2 . When we refer back to the chain rule (2.3.1) we notice that both terms are positive:

$$\begin{aligned} \frac{dS_1^*}{dS_2^*} &= \frac{\partial S_1^*}{\partial \alpha_{K,1}} \cdot \frac{d\alpha_{K,1}}{dS_2^*} + \frac{\partial S_1^*}{\partial \alpha_{P,1}} \cdot \frac{d\alpha_{P,1}}{dS_2^*} \\ \frac{dS_1^*}{dS_2^*} &= (-)(-) + (+)(+) \end{aligned}$$

This means that changes in S_1^* upon increases in S_2^* will always be positive. The increase in ultrasensitivity of S_2^* is thus transferred to S_1^* regardless of the values of the other parameters.

3 Analytical Results for the 1–Kinase/1–Phosphatase Loop with Many Substrates

The 1K1P loop can be expanded to include many substrates of the kinase and phosphatase. In this case we would have a system of enzymes such that:



where $E = K$ or P . From these equations we have:

$$[ES_1] = \frac{[E][S_1]}{K_{m,E,1}}, [ES_2] = \frac{[E][S_2]}{K_{m,E,2}}, \dots, [ES_N] = \frac{[E][S_N]}{K_{m,E,N}} \quad (3.1)$$

We also know from the conservation of mass of the enzyme:

$$[E]_0 = [E] + [ES_1] + [ES_2] + \dots + [ES_N] \quad (3.2)$$

Substituting the system of equations from 3.1 into 3.2, we get:

$$\begin{aligned}
 [E]_0 &= [E] \left(1 + \frac{[S_1]}{K_{m,E,1}} + \frac{[S_2]}{K_{m,E,2}} + \dots + \frac{[S_N]}{K_{m,E,N}} \right) \\
 [E] &= \frac{[E]_0}{1 + \frac{[S_1]}{K_{m,E,1}} + \frac{[S_2]}{K_{m,E,2}} + \dots + \frac{[S_N]}{K_{m,E,N}}} \\
 [ES_1] &= \frac{[E]_0[S_1]}{[S_1] + K_{m,E,1} \left(1 + \frac{[S_2]}{K_{m,E,2}} + \dots + \frac{[S_N]}{K_{m,E,N}} \right)} \quad (3.3)
 \end{aligned}$$

Substituting 3.3 into the previously defined 2.1.3, we arrive at:

$$\begin{aligned}
 \frac{d[S_1^*]}{dt} &= \frac{V_{max,1}[S_1]}{\alpha K_{m,E,1} + [S_1]} \\
 \alpha &\equiv 1 + \sum_{i=2}^N \frac{[S_i]}{K_{m,E,i}}
 \end{aligned}$$

From the above equation, we can proceed to solve for S_1^* as in section 2.2; as expected, one obtains equation 2.2.4, but with $\alpha_{K,1} \equiv 1 + \sum_{i=2}^N [S_i]/K_{m,K,i}$ and $\alpha_{P,1} \equiv 1 + \sum_{i=2}^N [S_i^*]/K_{m,P,i}$.

The increase in ultrasensitivity observed in Fig. 2B of the main text arises from the fact that, for the parameters we considered, at any $r_1 < 1$, the phosphatase has a higher maximum velocity

than the kinase. As such, the majority of any substrates present will exist in the unphosphorylated form (i.e. $S_i^* < 0.5 \forall i$). As more substrates are added, the accumulation of these unphosphorylated substrates begins to occupy the kinase, reducing free kinase concentration and thus reducing the “effective r ” of the system. In the limit where N is large, the occupation increases until the kinase is completely saturated, ultimately leading to very low phosphorylation at $r_1 < 1$. For $r_1 > 1$, a similar situation holds, but with the phosphatase occupied by the S_i^* ’s.

4 Analytical Results for the 1–Kinase/2–Phosphatase Loop

In this section we will show that S_1 phosphorylation always increases in $[S_2]_0$ in the limit in which $[S_1]_0 \ll K_m$. In this system S_1^* can be derived in a similar fashion to that for the 1K1P loop, resulting in:

$$S_1^* = \frac{(r_1 - 1) - (\alpha_{K,1}K_{K,1} + r_1K_{P,1}) + \sqrt{((r_1 - 1) - (\alpha_{K,1}K_{K,1} + r_1K_{P,1}))^2 + 4(r_1 - 1)r_1K_{P,1}}}{2(r_1 - 1)} \quad (4.0.1)$$

Note this is similar to 2.2.4, the difference being the absence of $\alpha_{P,1}$. This is because in this loop the substrates only share a kinase, making $\alpha_{P,1} = 1$. As such, $\frac{\partial S_1^*}{\partial \alpha_{P,1}} = 0$, by the chain rule we see:

$$\frac{dS_1^*}{d[S_2]_0} = \frac{dS_1^*}{d\alpha_{K,1}} \cdot \frac{d\alpha_{K,1}}{d[S_2]_0} \cdot \frac{d[S_2]}{d[S_2]_0} \quad (4.0.2)$$

Note that $\frac{dS_1^*}{d\alpha_{K,1}}$ is similar to $\frac{\partial S_1^*}{\partial \alpha_{K,1}}$ (2.3.4), the only difference being $\alpha_{P,1} = 1$ in this case. Since the value of $\alpha_{P,1}$ does not have an affect on the sign of $\frac{\partial S_1^*}{\partial \alpha_{K,1}}$, we can conclude that $\frac{dS_1^*}{d\alpha_{K,1}} < 0$ for any value of r_1 (see subsection 2.3). Additionally, we can easily show $\frac{d\alpha_{K,1}}{d[S_2]_0} > 0$:

$$\begin{aligned} \alpha_{K,1} &= 1 + \frac{[S_2]}{K_{m,K,2}} \\ \frac{d\alpha_{K,1}}{d[S_2]_0} &= \frac{1}{K_{m,K,2}} > 0 \end{aligned} \quad (4.0.3)$$

4.1 $d[S_2]/d[S_2]_0$ is always positive

Using Mathematica [3], we can obtain an expression for $\frac{d[S_2]}{d[S_2]_0}$ at $r_2 \neq 1$. To simplify the derivation, we assume $[S_1]_0 \ll K_m$ so that $\alpha_{K,2} = 1$.

$$\begin{aligned}
[S_2] &= (1 - S_2^*)[S_2]_0 \\
\frac{d[S_2]}{d[S_2]_0} &= 1 - S_2^* - \frac{dS_2^*}{d[S_2]_0}[S_2]_0 \\
&= 1 - \frac{-x' + \sqrt{(x')^2 + y'}}{2(r_2 - 1)} - \frac{z' + \frac{z'(-z') - \frac{y'}{2}}{\sqrt{(x')^2 + y'}}}{2(r_1 - 1)} \\
&= \frac{2(r_2 - 1) + x' - \sqrt{(x')^2 + y'} - z' + \frac{x'z' + \frac{y'}{2}}{\sqrt{(x')^2 + y'}}}{2(r_2 - 1)} \tag{4.1.1}
\end{aligned}$$

In which:

$$x' \equiv -((r_2 - 1) - (K_{K,2} + r_2 K_{P,2})), \quad y' \equiv 4(r_2 - 1)r_2 K_{P,2}, \quad z' \equiv K_{K,2} + r_2 K_{P,2} \tag{4.1.2}$$

By the definitions of x' and z' we notice that $x' = -(r_2 - 1) + z'$, which can be substituted into 4.1.1:

$$\begin{aligned}
\frac{d[S_2]}{d[S_2]_0} &= \frac{2(r_2 - 1) - (r_2 - 1) + z' - \sqrt{(x')^2 + y'} - z' + \frac{x'z' + \frac{y'}{2}}{\sqrt{(x')^2 + y'}}}{2(r_2 - 1)} \\
&= \frac{(r_2 - 1) - \sqrt{(x')^2 + y'} + \frac{x'z' + \frac{y'}{2}}{\sqrt{(x')^2 + y'}}}{2(r_2 - 1)} \\
&= \frac{(r_2 - 1)\sqrt{(x')^2 + y'} - (x')^2 - y' + x'z' + \frac{y'}{2}}{2(r_2 - 1)\sqrt{(x')^2 + y'}} \tag{4.1.3}
\end{aligned}$$

Additionally, by the definitions of x' and z' , we see $(x')^2 = (r_2 - 1)^2 - 2(r_2 - 1)z' + (z')^2$ and $x'z' = -(r_2 - 1)z' + (z')^2$, which can be substituted into 4.1.3:

$$\begin{aligned}
\frac{d[S_2]}{d[S_2]_0} &= \frac{(r_2 - 1)\sqrt{(x')^2 + y'} - (r_2 - 1)^2 + 2(r_2 - 1)z' - (z')^2 - (r_2 - 1)z' + (z')^2 - \frac{y'}{2}}{2(r_2 - 1)\sqrt{(x')^2 + y'}} \\
&= \frac{(r_2 - 1)\sqrt{(x')^2 + y'} - (r_2 - 1)^2 + (r_2 - 1)z' - \frac{y'}{2}}{2(r_2 - 1)\sqrt{(x')^2 + y'}} \\
&= \frac{\sqrt{(x')^2 + y'} - (r_2 - 1) + z' - 2r_2 K_{P,2}}{2\sqrt{(x')^2 + y'}} \\
&= \frac{\sqrt{(x')^2 + y'} + x' - 2r_2 K_{P,2}}{2\sqrt{(x')^2 + y'}} \tag{4.1.4}
\end{aligned}$$

We can show that $\frac{d[S_2]}{d[S_2]_0} > 0$ for all values of r_2 by assuming the opposite:

$$\begin{aligned} \frac{d[S_2]}{d[S_2]_0} &= \frac{\sqrt{(x')^2 + y'} + x' - 2r_2 K_{P,2}}{2\sqrt{(x')^2 + y'}} < 0 \\ \sqrt{(x')^2 + y'} + x' - 2r_2 K_{P,2} &< 0 \\ \sqrt{(x')^2 + y'} &< -x' + 2r_2 K_{P,2} \end{aligned} \quad (4.1.5)$$

If the right hand side of 4.1.5 is negative then we have already arrived at a contradiction. Otherwise we can square both sides without loss of information:

$$(x')^2 + y' < (x')^2 - 4r_2 K_{P,2} x' + 4(r_2 K_{P,2})^2 \quad (4.1.6)$$

$$\begin{aligned} y' &< -4r_2 K_{P,2} x' + 4(r_2 K_{P,2})^2 \\ 4(r_2 - 1)r_2 K_{P,2} &< 4(r_2 - 1)r_2 K_{P,2} - 4r_2 K_{K,2} K_{P,2} - 4(r_2 K_{P,2})^2 + 4(r_2 K_{P,2})^2 \\ 0 &< -4r_2 K_{K,2} K_{P,2} \end{aligned} \quad (4.1.7)$$

Which is clearly impossible, indicating $\frac{d[S_2]}{d[S_2]_0} > 0$ for $r_2 \neq 1$. Next we can obtain an expression for $\frac{d[S_2]}{d[S_2]_0}$ at $r_2 = 1$. At this point, S_2^* becomes:

$$S_2^* = \frac{K_{m,P,2}}{K_{m,K,2} + K_{m,P,2}} \quad (4.1.8)$$

As such, we can easily see that the derivative of 4.1.8 with respect to $[S_2]_0$ is equal to zero. Applying this to the previous expression for $\frac{d[S_2]}{d[S_2]_0}$ (4.1.1) we notice that at $r_2 = 1$:

$$\frac{d[S_2]}{d[S_2]_0} = 1 - S_2^* \quad (4.1.9)$$

Since S_2^* must be a value between 0 and 1, it is easy to see that $\frac{d[S_2]}{d[S_2]_0} > 0$ at $r_2 = 1$, thus showing that $\frac{d[S_2]}{d[S_2]_0} > 0$ for all values of r_2 .

4.2 $dS_1^*/d[S_2]_0$ is always negative

As previously shown, we can use the chain rule to define $\frac{dS_1^*}{d[S_2]_0}$ within this motif as:

$$\frac{dS_1^*}{d[S_2]_0} = \frac{dS_1^*}{d\alpha_{K,1}} \cdot \frac{d\alpha_{K,1}}{d[S_2]} \cdot \frac{d[S_2]}{d[S_2]_0} \quad (4.2.1)$$

In which $\frac{dS_1^*}{d\alpha_{K,1}} < 0$, $\frac{d\alpha_{K,1}}{d[S_2]} > 0$ and $\frac{d[S_2]}{d[S_2]_0} > 0$. Now we can see that $\frac{dS_1^*}{d[S_2]_0} < 0$ for all values of r_1 and r_2 . At $r_2 < 1$, $\alpha_{K,1} > 1$ as most S_2 will be in the unphosphorylated form. Once $r_2 > 1$, S_2 switches to its phosphorylated form, relieving the pressure on S_1 through $\alpha_{K,1}$, establishing the ‘‘gatekeeper’’ effect. We can see $\alpha_{K,1}$ approaches 1 as $r_2 \rightarrow \infty$, allowing S_1^* to behave as an isolated futile cycle in this limit. Since S_1^* is increasing in r_2 , we can conclude that S_2 decreases

S_1^* for all values of r_2 except in the limit $r_2 \rightarrow \infty$.

5 Analytical Results for the 2–Kinase/1–Phosphatase Loop

In this section we will show that S_1 phosphorylation also always increases in $[S_2]_0$ regardless of any other parameters. In this system S_1^* can be derived in a similar fashion to that for the 1K1P loop, resulting in:

$$S_1^* = \frac{(r_1 - 1) - (K_{K,1} + r_1\alpha_{P,1}K_{P,1}) + \sqrt{((r_1 - 1) - (K_{K,1} + r_1\alpha_{P,1}K_{P,1}))^2 + 4(r_1 - 1)r_1\alpha_{P,1}K_{P,1}}}{2(r_1 - 1)} \quad (5.0.1)$$

Which is equivalent to 2.2.4, the only difference being the lack of $\alpha_{K,1}$. As such $\frac{\partial S_1^*}{\partial \alpha_{K,1}} = 0$, and we notice that by the chain rule:

$$\frac{dS_1^*}{d[S_2]_0} = \frac{dS_1^*}{d\alpha_{P,1}} \cdot \frac{d\alpha_{P,1}}{d[S_2]_0} \cdot \frac{d[S_2^*]}{d[S_2]_0} \quad (5.0.2)$$

Note that $\frac{dS_1^*}{d\alpha_{P,1}}$ is similar to $\frac{\partial S_1^*}{\partial \alpha_{P,1}}$ (2.3.7), the only difference being $\alpha_{K,1} = 1$ in this case. Since the value of $\alpha_{K,1}$ does not have an affect on the sign of $\frac{\partial S_1^*}{\partial \alpha_{P,1}}$, we can conclude that $\frac{dS_1^*}{d\alpha_{P,1}} > 0$ for any value of r_1 (see subsection 2.3). Additionally, we can easily show $\frac{d\alpha_{P,1}}{d[S_2]_0} > 0$:

$$\begin{aligned} \alpha_{P,1} &= 1 + \frac{[S_2^*]}{K_{m,P,2}} \\ \frac{d\alpha_{P,1}}{d[S_2]_0} &= \frac{1}{K_{m,P,2}} \end{aligned} \quad (5.0.3)$$

5.1 $d[S_2^*]/d[S_2]_0$ is always positive

We can define $[S_2^*]$ as:

$$[S_2^*] = S_2^*[S_2]_0 \quad (5.1.1)$$

And as such $\frac{d[S_2^*]}{d[S_2]_0}$ is:

$$\frac{d[S_2^*]}{d[S_2]_0} = S_2^* + \frac{dS_2^*}{d[S_2]_0}[S_2]_0 \quad (5.1.2)$$

Notice that $\frac{d[S_2^*]}{d[S_2]_0} = 1 - \frac{d[S_2]}{d[S_2]_0}$ (see 4.1.1). We can then substitute 4.1.4 in for $\frac{d[S_2]}{d[S_2]_0}$:

$$\begin{aligned}\frac{d[S_2^*]}{d[S_2]_0} &= 1 - \frac{\sqrt{(x')^2 + y'} + x' - 2r_2 K_{P,2}}{2\sqrt{(x')^2 + y'}} \\ &= \frac{\sqrt{(x')^2 + y'} - x' + 2r_2 K_{P,2}}{2\sqrt{(x')^2 + y'}}\end{aligned}\tag{5.1.3}$$

We can show $\frac{d[S_2^*]}{d[S_2]_0} > 0$ for any value of r_2 by assuming the opposite:

$$\begin{aligned}\frac{d[S_2^*]}{d[S_2]_0} &= \frac{\sqrt{(x')^2 + y'} - x' + 2r_2 K_{P,2}}{2\sqrt{(x')^2 + y'}} < 0 \\ \sqrt{(x')^2 + y'} - x' + 2r_2 K_{P,2} &< 0 \\ \sqrt{(x')^2 + y'} &< x' - 2r_2 K_{P,2}\end{aligned}\tag{5.1.4}$$

If the right hand side of 5.1.4 is negative then we have already arrived at a contradiction. Otherwise we can square both sides without loss of information:

$$(x')^2 + y' < (x')^2 - 4r_2 K_{P,2} x' + 4(r_2 K_{P,2})^2\tag{5.1.5}$$

Note that this expression is the same as 4.1.6, which we have already shown to be impossible, supporting the conclusion $\frac{d[S_2^*]}{d[S_2]_0} > 0$ for $r_2 \neq 0$. Next we can obtain an expression for $\frac{d[S_2]}{d[S_2]_0}$ at $r_2 = 1$. At this point, S_2^* becomes:

$$S_2^* = \frac{K_{m,P,2}}{K_{m,K,2} + K_{m,P,2}}\tag{5.1.6}$$

As such, we can easily see that the derivative of 5.1.6 with respect to $[S_2]_0$ is equal to zero. Applying this to the previous expression for $\frac{d[S_2]}{d[S_2]_0}$ (5.1.2) we notice that at $r_2 = 1$:

$$\frac{d[S_2^*]}{d[S_2]_0} = S_2^*\tag{5.1.7}$$

Since S_2^* must be a value between 0 and 1, it is easy to see that $\frac{d[S_2^*]}{d[S_2]_0} > 0$ at $r_2 = 1$, thus showing that $\frac{d[S_2^*]}{d[S_2]_0} > 0$ for all values of r_2 .

5.2 $dS_1^*/d[S_2]_0$ is always positive

As previously shown, we can use the chain rule to define $\frac{dS_1^*}{d[S_2]_0}$ within this motif as:

$$\frac{dS_1^*}{d[S_2]_0} = \frac{dS_1^*}{d\alpha_{P,1}} \cdot \frac{d\alpha_{P,1}}{d[S_2^*]} \cdot \frac{d[S_2^*]}{d[S_2]_0}\tag{5.2.1}$$

In which $\frac{dS_1^*}{d\alpha_{P,1}} > 0$, $\frac{d\alpha_{P,1}}{d[S_2^*]} > 0$ and $\frac{d[S_2^*]}{d[S_2]_0} > 0$. Now we can see that $\frac{dS_1^*}{d[S_2]_0} > 0$ for all values of r_1 and r_2 .

References

1. Goldbeter A, K. D., 1981. An amplified sensitivity arising from covalent modification in biological systems. *Proc Natl Acad Sci U S A* 78:6840–44.
2. Nelson, D. L., and M. M. Cox, 2008. *Lehninger Principles of Biochemistry* 5th Edition.
3. Wolfram Research, I., 2010. *Mathematica*, Version 8.0. Champaign, Illinois.